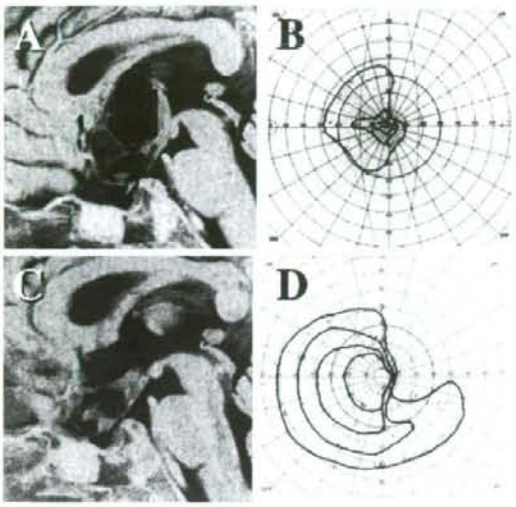

Fig. 5. A multicystic expansion of a pilocytic astrocytoma after 9-year remission following initial chemotherapy and radiation therapy (A). The visual function was deteriorated (B). A partial removal of the cyst wall by a craniotomy achieved collapse of most of the cysts (C) and improvement of vision (D).

had been stable. The visual function of this 10-year-old patient was rapidly deteriorating. Partial removal of the cyst wall by craniotomy resulted in collapse of most of the cysts and improvement in the patient's vision. A selective resection of cystic walls preserving the remaining optic pathway always requires precise presurgical MRI investigation with three-dimensional MR cisternography and careful surgical planning.

Discussion

All 25 children tolerated the various therapies well, and all were alive at the time of final observation. Among them, only one patient definitely achieved a tumor-free status. The long-term final outcome of these patients will be clearer 10 or more years after this report. Therefore, we here focus on the efficacy of the surgical interventions.

Biopsy at the Initiation of Therapy

In 1995, Sutton et al.[14] reported the long-term outcome of hypothalamic/chiasmatic astrocytomas in children treated with conservative surgery. In their series, all patients who had globular suprasellar masses without involvement of optic nerves or optic radiations underwent surgical exploration. The goal of this surgery was primarily to establish a histological diagnosis, and if a typical low-grade astrocytoma was encountered, a biopsy and limited resection were performed. Large masses obstructing the foramen of Monro were debulked to relieve ventricular obstruction, but generally no attempt at gross total excision was made. This concept may have been widely accepted as a standard surgical strategy for OPHPA at initial treatment.[3,21]

Currently, OPHPA in children with usual clinical and radiographic appearance using modern MRI technique can be more correctly diagnosed without surgical biopsy. The majority of such patients respond to platinum-based chemotherapy.[3–7,9–11] Serious visual dysfunction can be improved by chemotherapy, and a chemotherapy-first strategy can preserve the intellectual outcome of patients who thereby avoid the need for radiotherapy.[22,23] In our series, 11 biopsies (limited resections) by craniotomy in fact caused remarkable complications related to surgical procedure. We speculate that these were attributable to incorrect preoperative diagnosis or insufficient experience of the surgeon. For example, two young children had a preoperative diagnosis of craniopharyngioma; however, pilocytic astrocytoma was suggested by frozen section during the craniotomy. In these children, a bifrontal interhemispheric approach by a large craniotomy was used; nevertheless, the surgery produced unnecessary complications. In contrast to chemotherapy, the result of surgical intervention depends on the surgeon's skill and experience. The benefit of surgical biopsy at initiation of therapy may therefore be ambiguous considering surgical morbidities, cost, and delay of chemotherapy. Silva et al.[11] treated 14 young children, including four patients after endoscopic biopsy and five patients without biopsy, and recommended chemotherapy as a primary treatment for optic pathway/hypothalamic gliomas.

Gliomas in similar locations, such as NF-1–associated gliomas, single optic nerve gliomas, hypothalamic hamartomas, and unilateral hypothalamic gliomas, require a treatment strategy distinct from that for OPHPA. Excluding these instances by MRI examination, the vast majority of gliomas involving the optic pathway and bilateral hypothalamus in children are pilocytic astrocytomas.[8,14,24] Other tumors in the same region, however, may mimic OPHPA and would necessitate different therapeutic approaches. In addition to routine imaging studies and endocrinological assessments, examinations of tumor markers in the serum and cerebrospinal fluid and high-resolution MR images, such as MR cisternography or multiple planner reconstruction image, should suitably assist the diagnosis, to rule out craniopharyngioma, various germ cell tumors, Langerhans cell histiocytosis, hypothalamic hamartoma, diffuse astrocytoma, or ganglioglioma. In some cases, surgical biopsy is indispensable to confirm histological diagnosis. In some instances, image-guided stereotactic biopsy or endoscopic biopsy may be feasible and valuable. These procedures carry some risk, and difficulty may be experienced in small children without dilatation of lateral ventricles.

Pilomyxoid astrocytoma, an infantile variant with known aggressive potential, may be more susceptible to chemotherapy and exhibit more typical features on MRI compared with classical pilocytic astrocytomas found in older children,[2,4,6–10,15,21,24] given that children younger than 1 year have a higher risk for tumor progression than do older children.[6,8,15,17] The surgical risk of cran-

iotomy for very small children is clearly high. Furthermore, a combination of surgical operation and histological examination may delay initiation of chemotherapy. Moreover, surgical removal might introduce tumor cell seeds into the cerebrospinal fluid pathway. There may be no place for surgical exploration in the treatment of young children, except for endoscopic biopsy.

Partial Resection at the Initiation of Therapy

In addition to the use of biopsy for diagnosis, some investigators have advocated resection for large tumors, and certain children can obtain long-term amelioration by initial surgical resection alone.[16,17] In 2002, Steinbok et al.[25] reported surgical results for 18 chiasmatic-hypothalamic astrocytomas; eight patients had subtotal resections, six had partial resections, three had limited resections, and one had no surgery. Fewer complications were associated with the limited resections, especially with respect to hypothalamic dysfunction. There was no correlation between the extent of resection and the time to tumor progression. The chiasmatic-hypothalamic tumors caused more morbidity than did the chiasmatic tumors, and radical resections did not prolong time to progression compared with more limited resections. The authors concluded that if surgery is performed, it may be appropriate to do a surgical procedure that strives only to provide a tissue diagnosis and to decompress the optic apparatus and/or ventricular system.

We agree with the conclusion of Steinbok et al.[25] Selective decompression of the optic apparatus, however, appeared to be difficult. Precise estimation of visual dysfunction as a consequence of partial resection is difficult to nearly impossible, especially in young children. Surgical morbidity in the previous reports might have been underestimated with respect to visual function in children. In addition, as demonstrated in Fig. 1, if the tumor is located mainly in the chiasm, a partial excision of the tumor will injure the visual pathway.

Concerning the complications and invasiveness of such debulking surgery, decompression of the ventricular system by a partial resection can be replaced with a ventriculoperitoneal shunt, with or without endoscopic septotomy. Only when chemotherapy fails to induce or maintain remission should salvage debulking surgery be planned.

Salvage Resection Surgery

Chemotherapy is increasingly being used and is occasionally curative, and it provides a stabilizing role in most cases.[3,6,8,9,11] Following initial induction chemotherapy, even if it was effective and given for a long period, many children with OPHPA experience tumor relapse. The second-line treatment may be alternative chemotherapy, and radiation therapy might then be considered at further progression.[6] Because the long-term effectiveness of conventional fractionated radiation therapy, including recent stereotactic techniques, is superior to that of chemotherapy,[3,26–28] radiation therapy is available for older children with a localized relapse. However, some OPHPAs are "surgically amenable" in a subset of patients with recurrent disease.[14,17]

It is known that optic gliomas in non-NF-1 patients often regress spontaneously.[13,17,29] If most pilocytic astrocytomas have a limited time span for growing and lower age is a worse prognostic factor,[8,21,30] a partial resection to ameliorate symptoms or to reduce mass effect of a growing tumor may be worthwhile. In our series of patients, spontaneous involution after partial resection or cyst puncture of a relapsing tumor was observed in four patients. This result may warrant a salvage maximal (partial) excision for relapsing tumor with parenchymal growth, especially in older children.

Radical Surgery and Complication

Radical surgery for patients with OPHPA carries the risk of damage to the hypothalamus, visual apparatus, and vascular structures.[17] In addition, no complete surgical resection could be achieved when the functional outcome was seriously considered.[2,14,24] Neurosurgeons, however, seldom have the opportunity to operate on OPHPA, which is an uncommon childhood brain tumor. In addition, the surgical strategy and technique are extremely complex. In our series of patients, the complication rates from biopsy and bulk-reduction surgery at the initiation of therapy seemed to be unexpectedly high compared with literature reports.[2,3,11,14,17,21] Definitive permanent deficits occurred in two children after 11 open biopsies and in four children after 7 bulk-reduction surgeries. Few of these complications, however, resulted from the surgeries performed by the senior author, suggesting an effect of surgeon experience.

It is of note that results of such surgical excisions may vary and that the results greatly depend on the experience of the neurosurgeon. Although OPHPA should be operated on by an experienced surgeon, results will vary with the specific conditions in each case. Radical surgical resection of OPHPA will therefore generally be offered only when the tumor has progressed despite feasible chemotherapy or, in certain cases, radiation therapy.

Partial Removal for Cystic Expansion

Cystic tumor expansion without parenchymal growth occurred mostly in older children. The formation of cysts may be a consequence of tumor degeneration and may occur prior to spontaneous involution, as observed in cases of vestibular schwannoma. The growing cyst (containing proteinaceous fluid) appeared to be refractory to both chemotherapy and radiation therapy. An intended nonaggressive partial resection of cyst wall(s) or stereotactic puncture can ameliorate progressive visual disturbance and produce a certain term of remission.

Optic Nerve Decompression

OPHPA occasionally involves the optic nerves in the optic canal. The swollen optic nerve expands the bony optic canal, especially in very young children (younger than ~4 years of age) and may result in entrapment neu-

ropathy of the optic nerve itself. To our knowledge, no report has described the efficacy of optic nerve decompression for such cases. Although we had a solitary case of successful decompression in the present series, this surgical procedure may be applied to rescue very poor vision caused by optic nerve invasion by tumor cells.

In conclusion, to treat OPHPA in young children, surgical biopsy appears to be dispensable for clinically or radiologically typical cases. A curative resection is rarely achieved when the functional outcome of patients is seriously respected. The role of surgical intervention may be restricted to bulk-reduction surgery only when it is inevitable. However, during the long clinical course of OPHPA in children, especially at relapse, both chemotherapy and radiation therapy have to be selected considering a variety of available surgical treatments with neurosurgeons who have profound experience with this unique tumor.

Acknowledgment

This study was supported partly by Clinical Cancer Research and Health and Labor Sciences research grants (H17-ganrinsyou-ippan-005) from the Ministry of Health, Labour and Welfare.

References

1. Chikai K, Ohnishi A, Kato T, et al. Clinico-pathological features of pilomyxoid astrocytoma of the optic pathway. *Acta Neuropathol (Berl).* 2004;108:109–114.
2. Fernandez C, Figarella-Branger D, Girard N, et al. Pilocytic astrocytomas in children: prognostic factors—a retrospective study of 80 cases. *Neurosurgery.* 2003;53:544–555.
3. Fouladi M, Wallace D, Langston JW, et al. Survival and functional outcome of children with hypothalamic/chiasmatic tumors. *Cancer.* 2003;97:1084–1092.
4. Gururangan S, Cavazos CM, Ashley D, et al. Phase II study of carboplatin in children with progressive low-grade gliomas. *J Clin Oncol.* 2002;13:2951–2958.
5. Kato T, Sawamura Y, Tada M, Ikeda J, Ishii N, Abe H. Cisplatin/vincristine chemotherapy for hypothalamic/visual pathway astrocytomas in young children. *J Neurooncol.* 1998;37:263–270.
6. Laithier V, Grill J, Le Deley MC, et al. Progression-free survival in children with optic pathway tumors: dependence on age and the quality of the response to chemotherapy—results of the first French prospective study for the French Society of Pediatric Oncology. *J Clin Oncol.* 2003;21:4572–4578.
7. Massimino M, Spreafico F, Cefalo G, et al. High response rate to cisplatin/etoposide regimen in childhood low-grade glioma. *J Clin Oncol.* 2002;20:4209–4216.
8. Opocher E, Kremer LC, Da Dalt L, et al. Prognostic factors for progression of childhood optic pathway glioma: a systematic review. *Eur J Cancer.* 2006;42:1807–1816.
9. Packer RJ, Ater J, Allen J, et al. Carboplatin and vincristine chemotherapy for children with newly diagnosed progressive low-grade gliomas. *J Neurosurg.* 1997;86:747–754.
10. Packer RJ, Sutton LN, Bilaniuk LT, et al. Treatment of chiasmatic/hypothalamic gliomas of childhood with chemotherapy: an update. *Ann Neurol.* 1988;23:79–85.
11. Silva MM, Goldman S, Keating G, Marymont MA, Kalapurakal J, Tomita T. Optic pathway hypothalamic gliomas in children under three years of age: the role of chemotherapy. *Pediatr Neurosurg.* 2000;33:151–158.
12. Strong JA, Hatten HP Jr, Brown MT, et al. Pilocytic astrocytoma: correlation between the initial imaging features and clinical aggressiveness. *AJR Am J Roentgenol.* 1993;161:369–372.
13. Suarez JC, Viano JC, Zunino S. Management of child optic pathway gliomas: new therapeutical option. *Childs Nerv Syst.* 2006;22:679–684.
14. Sutton LN, Molloy PT, Sernyak H, et al. Long-term outcome of hypothalamic/chiasmatic astrocytomas in children treated with conservative surgery. *J Neurosurg.* 1995;83:583–589.
15. Tihan T, Fisher PG, Kepner JL, et al. Pediatric astrocytomas with monomorphous pilomyxoid features and a less favorable outcome. *J Neuropathol Exp Neurol.* 1999;58:1061–1068.
16. Hoffman HJ, Humphreys RP, Drake JM, et al. Optic pathway/hypothalamic gliomas: a dilemma in management. *Pediatr Neurosurg.* 1993;19:186–195.
17. Wisoff JH, Abbott R, Epstein F. Surgical management of exophytic chiasmatic-hypothalamic tumors of childhood. *J Neurosurg.* 1990;73:661–667.
18. Grill J, Laithier V, Rodriguez D, Raquin MA, Pierre-Kahn A, Kalifa C. When do children with optic pathway tumours need treatment? An oncological perspective in 106 patients treated in a single centre. *Eur J Pediatr.* 2000;159:692–696.
19. Leonard JR, Perry A, Rubin JB, King AA, Chicoine MR, Gutmann DH. The role of surgical biopsy in the diagnosis of glioma in individuals with neurofibromatosis-1. *Neurology.* 2006;67:1509–1512.
20. Therasse P, Arbuck SG, Eisenhauer EA, et al. New guidelines to evaluate the response to treatment in solid tumors. *J Natl Cancer Inst.* 2000;92:205–216.
21. Chan MY, Foong AP, Heisey DM, Harkness W, Hayward R, Michalski A. Potential prognostic factors of relapse-free survival in childhood optic pathway glioma: a multivariate analysis. *Pediatr Neurosurg.* 1998;29:23–28.
22. Lacaze E, Kieffer V, Streri A, et al. Neuropsychological outcome in children with optic pathway tumours when first-line treatment is chemotherapy. *Br J Cancer.* 2003;89:2038–2044.
23. Mitchell AE, Elder JE, Mackey DA, Waters KD, Ashley DM. Visual improvement despite radiologically stable disease after treatment with carboplatin in children with progressive low-grade optic/thalamic gliomas. *J Pediatr Hematol Oncol.* 2001;23:572–577.
24. Komotar RJ, Burger PC, Carson BS, et al. Pilocytic and pilomyxoid hypothalamic/chiasmatic astrocytomas. *Neurosurgery.* 2004;54:72–79.
25. Steinbok P, Hentschel S, Almqvist P, Cochrane DD, Poskitt K. Management of optic chiasmatic/hypothalamic astrocytomas in children. *Can J Neurol Sci.* 2002;29:132–138.
26. Erkal HS, Serin M, Cakmak A. Management of optic pathway and chiasmatic-hypothalamic gliomas in children with radiation therapy. *Radiother Oncol.* 1997;45:11–15.

27. Gnekow AK, Kortmann RD, Pietsch T, Emser A. Low grade chiasmatic-hypothalamic glioma-carboplatin and vincristin chemotherapy effectively defers radiotherapy within a comprehensive treatment strategy—report from the multicenter treatment study for children and adolescents with a low grade glioma—HIT-LGG 1996—of the Society of Pediatric Oncology and Hematology (GPOH). *Klin Padiatr.* 2004;216:331–342.

28. Marcus KJ, Goumnerova L, Billett AL, et al. Stereotactic radiotherapy for localized low-grade gliomas in children: final results of a prospective trial. *Int J Radiat Oncol Biol Phys.* 2005;61:374–379.

29. Parsa CF, Hoyt CS, Lesser RL, et al. Spontaneous regression of optic gliomas: thirteen cases documented by serial neuroimaging. *Arch Ophthalmol.* 2001;119:516–529.

30. Palma L, Celli P, Mariottini A. Long-term follow-up of childhood cerebellar astrocytomas after incomplete resection with particular reference to arrested growth or spontaneous tumour regression. *Acta Neurochir (Wien).* 2004;146:581–588.

Association of p16 Homozygous Deletions with Clinicopathologic Characteristics and EGFR/KRAS/p53 Mutations in Lung Adenocarcinoma

Reika Iwakawa,[1,6] Takashi Kohno,[1] Yoichi Anami,[4] Masayuki Noguchi,[4] Kenji Suzuki,[2] Yoshihiro Matsuno,[3] Kazuhiko Mishima,[5] Ryo Nishikawa,[5] Fumio Tashiro,[6] and Jun Yokota[1]

Abstract **Purpose:** The *p16* gene is frequently inactivated in lung adenocarcinoma. In particular, homozygous deletions (HD) have been frequently detected in cell lines; however, their frequency and specificity is not well-established in primary tumors. The purpose of this study was to elucidate the prevalence and the timing for the occurrence of p16 HDs in lung adenocarcinoma progression *in vivo*.

Experimental Design: Multiple ligation-dependent probe amplification was used for the detection of p16 HDs in 28 primary small-sized lung adenocarcinomas and 22 metastatic lung adenocarcinomas to the brain. Cancer cells were isolated from primary adenocarcinoma specimens by laser capture microdissection. HDs were confirmed by quantitative real-time genomic PCR analysis.

Results: HDs were detected in 8 of 28 (29%) primary tumors, including 2 of 8 (25%) noninvasive bronchioloalveolar carcinomas, and 5 of 22 (26%) brain metastases, respectively. No significant associations were observed between p16 HDs and gender, age, smoking history, stage, and prognosis. HDs were detected with similar frequencies (17–29%) among adenocarcinomas with epidermal growth factor receptor (EGFR) mutations, with KRAS mutations, and without EGFR/KRAS mutations, and with similar frequencies (22–28%) between adenocarcinomas with and without p53 mutations.

Conclusions: p16 HDs occur early in the development of lung adenocarcinomas and with similar frequencies among EGFR type, KRAS type, and non-EGFR/KRAS type lung adenocarcinomas. Tobacco carcinogens would not be a major factor inducing p16 HDs in lung adenocarcinoma progression.

Adenocarcinoma is the most common histologic type of lung cancer. Recent molecular analyses have indicated that lung adenocarcinoma can be divided into at least three types; the epidermal growth factor receptor (EGFR) type, the KRAS type, and the non-EGFR/KRAS type, based on accumulated genetic alterations in adenocarcinoma cells (1, 2). The *p16* tumor suppressor gene is frequently inactivated in lung adenocarcinomas, most prominently through promoter methylation and homozygous deletion (HD), and less frequently through intragenic mutation (3–6). In particular, p16 methylation is known to occur in close association with tobacco carcinogen exposure and preferentially in the KRAS type adenocarcinomas (1). Molecular analyses of small-sized adenocarcinomas revealed that p16 methylation occurs in the course of progression from noninvasive bronchioloalveolar carcinomas (BAC) to invasive ones, and its occurrence is associated with smoking history, staging, and prognosis (7). However, it is still unknown whether p16 HD also occurs preferentially in the KRAS type or not. In addition, the involvement of tobacco smoking in the occurrence of p16 HD is also unclear because both positive and negative associations between tobacco smoking and HD have been reported (5, 6). Indeed, p16 HDs have been reported to occur with a highly variable frequency in primary lung adenocarcinomas (0–40%; refs. 3–6, 8). HD can be easily masked if a large fraction of noncancerous cells are contaminated in tumor tissues, in particular, in the analysis of small tumors with a BAC component. Thus, such an inconsistency could come not only from the diversity and/or heterogeneity of lung adenocarcinomas but also from tumor tissues used for the analysis and also from the methods used for the detection of HDs. For instance, immunohistochemical analyses of p16 proteins have shown that a considerable

Authors' Affiliations: [1]Biology Division, National Cancer Center Research Institute, [2]Thoracic Surgery Division and [3]Diagnostic Pathology Division, National Cancer Center Hospital, Tokyo, Japan; [4]Department of Pathology, Institute of Basic Medical Sciences, Graduate School of Comprehensive Human Sciences, Tsukuba University, Ibaraki, Japan; [5]Department of Neuro-Oncology, Comprehensive Cancer Center, International Medical Center, Saitama Medical University, Saitama, Japan; and [6]Department of Biological Science and Technology, Faculty of Industrial Science and Technology, Tokyo University of Science, Chiba, Japan

Received 10/5/07; revised 2/24/08; accepted 2/28/08.

Grant support: Grants-in-Aid from the Ministry of Health, Labor and Welfare for the Third-Term Comprehensive 10-Year Strategy for Cancer Control and for Cancer Research (16-1) and a Grant-in-Aid for the Program for Promotion of Fundamental Studies in Health Sciences of the National Institute of Biomedical Innovation (NiBio).

The costs of publication of this article were defrayed in part by the payment of page charges. This article must therefore be hereby marked *advertisement* in accordance with 18 U.S.C. Section 1734 solely to indicate this fact.

Requests for reprints: Jun Yokota, Biology Division, National Cancer Center Research Institute, 1-1, Tsukiji 5-chome, Chuo-ku, Tokyo 104-0045, Japan. Phone: 81-33547-5272; Fax: 81-33542-0807; E-mail: jyokota@ncc.go.jp.

doi:10.1158/1078-0432.CCR-07-4552

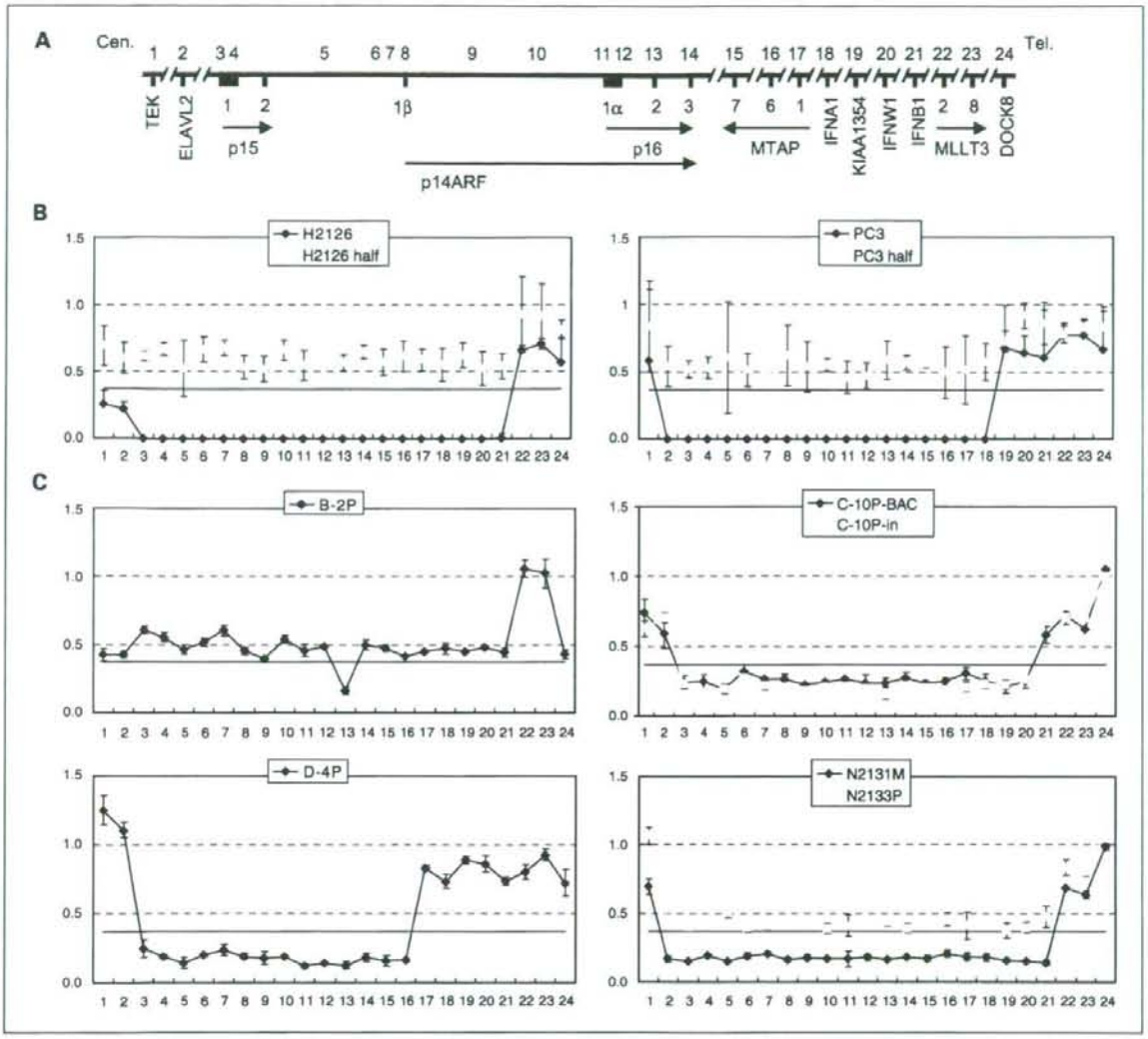

Fig. 1. HDs of the *p16* gene detected by MLPA analysis. *A*, physical map of the chromosome 9p region. Top, positions of 24 probes from nos. 1 to 24 (*red*) in the order from centromere (*Cen.*) to telomere (*Tel.*). Bottom, positions of 12 genes in this region (*light blue*). Exons (*numbers*) and orientations (*arrows*) of the *p15, p14ARF, p16, MTAP,* and *MLLT3* genes. *B*, definition of p16 HDs by MLPA analysis. Relative copy numbers of the 24 loci in two lung adenocarcinoma cell lines, H2126 and PC3 (*blue dots/lines*), and those in mixed samples of the same amounts of DNA from these cell lines and normal lung tissue (*pink dots/lines*; H2126 half and PC3 half, respectively). *C*, results of MLPA analysis for cases B-2P, C-10P, D-4P, and N2131M/N2133P showing HDs of the *p16* gene. As for case C-10P, both the BAC component (*BAC; blue dots/lines*) and the invasive region (*in; pink dots/lines*) of the tumor were analyzed. N2131M (*blue*) and N2133P (*pink*) are a brain metastasis and the primary tumor from the same patient, respectively.

fraction of adenocarcinomas are negative for p16 protein expression without clear evidence of an inactivating event by molecular analyses of the *p16* gene (4, 5, 7). Thus, it has been assumed that p16 HD is a causative event for the absence of p16 protein in these adenocarcinoma cases. However, due to the lack of comprehensive analysis for p16 HDs, the prevalence, specificity, and the timing for the occurrence of p16 HDs in lung adenocarcinoma progression *in vivo* is still unclear.

In this study, we investigated the association of p16 HDs with clinicopathologic characteristics, including smoking history, of lung adenocarcinomas and with the status of EGFR, KRAS, and p53 mutations in lung adenocarcinomas. To obtain more critical information than previous studies for the timing of its occurrence in the progression of lung adenocarcinomas, we analyzed two typical stages of lung adenocarcinomas. One is a primary small-sized adenocarcinoma of ≤2 cm in maximum diameter as a representative of early stage lung adenocarcinomas, and the other is a brain metastasis as a representative of late stage lung adenocarcinomas. To exclude the possible overlooking of HDs in the analysis due to contamination of noncancerous cells in tumor tissues, a laser capture

microdissection method was applied for the isolation of cancer cells from small-sized primary lung adenocarcinomas. Brain metastases are known to be relatively solid and generally contain a small amount of noncancerous cells in tumor tissues; therefore, macrodissected samples were used for the analysis. Recently, a simple and effective method, which is called multiplex ligation-dependent probe amplification (MLPA), to measure the copy number of up to 45 genomic loci in a single experiment, was developed and has been applied for the detection of large deletions in/of various genes in the human genome DNA sequence (9). For instance, this method was successfully applied for the detection of p16 hemizygous deletions in melanoma families (10) and p16 HDs in head and neck squamous cell carcinoma cell lines (11). Thus, we applied this method for the detection of p16 HDs in surgically resected lung adenocarcinomas. HDs were detected with similar frequencies of 23% to 40% in lung adenocarcinomas of any progression stage—from noninvasive carcinomas to advanced ones. The deletions were also detected with similar frequencies among EGFR type, KRAS type, and non-EGFR/KRAS type adenocarcinomas, and were not associated with tobacco smoking and poor prognosis.

Materials and Methods

Patients and tissues. Twenty-eight primary small-sized (≤2 cm in maximum diameter) adenocarcinomas, 22 brain metastases, and corresponding noncancerous tissues were obtained at surgery from lung adenocarcinoma patients treated at the National Cancer Center Hospital, Tokyo and at the Saitama Medical University. In 4 of the 22 brain metastasis cases, the corresponding primary tumors were also obtained at surgery. The surgically resected specimens were fixed routinely with 10% formalin and embedded in paraffin for histologic examination. All the sections were stained with H&E and examined by light microscopy. The tumors were pathologically diagnosed according to the tumor-node-metastasis classification of malignant tumors (12). The primary small-sized adenocarcinomas were further classified into three types according to the histologic classification of small-sized adenocarcinoma of the lung reported by Noguchi and colleagues (13), and there were 8 type B, 15 type C, and 5 type D adenocarcinomas. These 28 tumors and corresponding noncancerous tissues were fixed with methanol and embedded in paraffin. Cancer cells were then microdissected using the Pixcell Laser Capture Microdissection system (Arcturus Engineering), and their genomic DNAs were extracted as described previously (14). Representative figures of type B and C tumors before and after microdissection have been shown in our previous article (14). All of the 22 brain metastases, corresponding primary tumors, and noncancerous tissues were macrodissected and stored at -80°C until DNA extraction. Genomic DNAs were prepared as previously described (15).

Cell lines. Three lung adenocarcinoma cell lines, H2126, A549, and PC3, were used as positive controls of p16 HDs in MLPA and quantitative real-time genomic PCR (QRT-G-PCR) analysis. Genomic DNA were prepared as previously described (15). Incidence as well as regions of p16 HDs in 55 lung adenocarcinoma cell lines, including these three cell lines, were determined by multiplex PCR analysis in our previous studies (3).

MLPA analysis. MLPA was carried out using the P024B kit for the 9p21 CDKN2A/2B region (MRC-Holland) according to the manufacturer's protocol. The kit contains 12 probes covering the *p15/p14ARF/p16* genes, 12 probes for 9 other genes on chromosome 9p, and 15 control probes for nonchromosome 9p loci. Genes on chromosome 9p included in this screen were *TEK, ELAVL2, CDKN2B (p15), CDKN2A (p14ARF/p16), MTAP, IFNA1, KIAA1354, IFNW1, IFNB1, MLLT3,* and *DOCK8 (FLJ00026)* in the order from centromere to telomere (Fig. 1A). Experiments were done in a half volume until the ligation reaction step, and then by the supplied protocol. Briefly, 12.5 to 50 ng of genomic DNA in 2.5 to 5 μL of TE buffer were heat-denatured and hybridized to probes for 16 h at 60°C. The hybridized probes were then ligated and amplified by PCR of 35 cycles at 60°C for 30 s and 72°C for 60 s. PCR products were separated by capillary electrophoresis using the ABI3700 Automated Capillary DNA Sequencer with a 50-cm capillary array, ABI POP-6 polymer, and GeneScan-ROX 500 size standards (Applied Biosystems). Analysis was automated using ABI PRISM GeneScan Analysis software version 3.7, and Genotyper Analysis software version 3.7 (Applied Biosystems). PCR and electrophoresis, respectively, were done in duplicate, and the mean of four values was calculated and considered to be the DNA copy number ratio of each locus.

Data analysis. The relative DNA copy number of each locus was calculated as follows. First, the value for the sum of 15 autosomal control probe peak areas in a lung adenocarcinoma sample was adjusted to the mean value for those in two or three normal lung tissue samples in the same run. Each of the 39 probe peak areas was then divided by the sum of the peak areas of the 15 autosomal control probe peak areas. Finally, the relative DNA copy number ratio of each of the 39 chromosome loci in the lung adenocarcinoma samples against the normal lung tissue samples was calculated. Theoretically, ratios close to 1.0 indicated that two DNA copies were present (i.e., wild-type), a ratio of 0.5 indicated that one copy was absent (i.e., hemizygous deletion), and a ratio of 0.0 indicated that both copies were absent (i.e., homozygous deletion). The criteria for hemizygous deletions and HDs of the 39 loci by MLPA analysis were defined using MLPA data from three lung adenocarcinoma cell lines with p16 HDs as described in Results and Discussion. The *p16* gene was then defined as homozygously deleted or not in each sample. Because the purpose of this study is to evaluate the prevalence of p16 HD, hemizygous deletions were not evaluated from MLPA data.

QRT-G-PCR analysis. TaqMan-MGB probes and primers were designed using Primer Express software (Applied Biosystems) and were optimized according to the manufacturer's guidelines. Target and reference locus probes were labeled with FAM and VIC, respectively. Probe sequences were as follows: no. 9, 5′-AACTCCTCCACTGATTAC-3′; and 2p14, 5′-CCAGCCTATTCCTGC-3′. Primer sequences were as follows: no. 9-F/R, 5′-GGGTCTCCTTCATTTGGTGAAA-3′/5′-GGATCCCAGGGAGGAGAGTCT-3′; and 2p14-F/R, 5′-AAGAAGACTGGAGTGGTGTTTGG-3′/5′-CACAATGCTGAATACTGTCAATGAAA-3′. PCR was carried out in duplicate using 1 ng of DNA as a template. Primer and probe concentrations were optimized for each target according to the manufacturer's instructions. The PCR program consisted of 50°C for 2 min and 95°C for 15 min followed by 45 cycles of 95°C for 15 s and 60°C for 1 min. Standard curves for the copy numbers of the target and reference genes were generated using serially diluted (0.04–25 ng) normal lung tissue DNA. Data analysis was carried out using ABI Prism 7900HT Sequence Detection Software. DNA copy number ratios were calculated as the average copy number of the target locus divided by the average copy number of the reference locus, and then normalized against the normal lung tissue DNA to give a normalized DNA copy number ratio.

Immunohistochemistry. Immunohistochemical analysis of p16 protein was performed as described previously (7) using 4-μm sections cut from methanol-fixed and paraffin-embedded specimens of 28 primary small-sized adenocarcinomas, which were subjected to MLPA analysis. Positivity for p16 staining was scored by the same criteria as previously described (7). In brief, only nuclear staining was scored, and was considered to be positive when it was more intense than the background cytoplasmic staining. If <10% of tumor cells displayed p16 protein staining, it was judged negative; and if >10% of them showed strong staining, it was judged positive.

Mutation analysis of the* EGFR, KRAS, *and* p53 *genes. Thirteen of the 28 primary tumors, and 16 of the 22 brain metastases were

Table 1. Frequencies of p16 HDs and EGFR/KRAS/p53 mutations in lung adenocarcinoma

Sample	Subtype	Frequency (%)			
		p16	EGFR	KRAS	p53
Surgical specimen		13/50 (26)	34/50 (68)	4/50 (8)	32/50 (64)
Primary tumor		8/28 (29)	21/28 (75)	2/28 (7)	16/28 (57)
	Type B	2/8 (25)	8/8 (100)	0/8 (0)	2/8 (25)
	Type C	4/15 (27)	12/15 (80)	1/15 (7)	9/15 (60)
	Type D	2/5 (40)	1/5 (20)	1/5 (20)	5/5 (100)
Brain metastasis		5/22 (23)	13/22 (59)	2/22 (9)	16/22 (73)
Cell line*		20/55 (36)	-	-	-

*Defined in our previous study (17).

previously examined for mutations of exons 18 to 21 in the *EGFR* gene, of exons 1 and 2 in the *KRAS* gene, and of exons 4 to 8 in the *p53* gene by genomic PCR and direct sequencing (14, 16). The remaining 15 primary tumors and 6 brain metastases were also examined for these mutations in this study using the same methods.

Statistical analysis. Fisher's exact test was used to assess the association of p16 HDs with clinicopathologic characteristics or mutations of the *EGFR*, *KRAS*, and *p53* genes. $P < 0.05$ was considered to be statistically significant.

Results and Discussion

Detection of HDs by MLPA analysis. We previously determined regions of p16 HDs in various lung cancer cell lines by multiplex genomic PCR analysis (3, 17). Thus, we first validated the sensitivity and specificity of the MLPA method to detect p16 HDs using several lung adenocarcinoma cell lines. No PCR amplification was observed for probes that hybridized to the sequences of HD regions in all the cell lines examined. Representative results of MLPA analysis for two cell lines, H2126 and PC3, are shown in Fig. 1B. We then applied MLPA analysis for the detection of p16 HDs in surgically resected adenocarcinoma samples. Cancer cells of small-sized primary adenocarcinomas were isolated by laser capture microdissection, and brain metastases generally contain a small fraction of noncancerous cells. However, a complete absence of PCR products was not observed for these samples at any chromosomal loci by MLPA analysis. Therefore, we next defined the criteria for p16 HDs by MLPA analysis for surgically resected samples. For this purpose, DNA samples with virtual hemizygous deletions were prepared by mixing the same amounts of DNA from normal lung tissue and from three lung cancer cell lines with p16 HDs, H2126, A549, and PC3. In total, 64 probe loci were homozygously deleted in these cell lines. The mean ± 3 SD of relative DNA copy number ratios for the 64 probe loci in the HD regions among these mixed samples was 0.54 ± 0.17; thus, the range of virtual hemizygous deletions was 0.37 to 0.71. Indeed, none of the 64 probe loci in the HD regions of the mixed samples showed a DNA copy number ratio of >0.71 or <0.37 (Fig. 1B). Therefore, if the DNA copy number ratio for a locus was <0.37, the locus was judged as homozygously deleted in surgically resected lung adenocarcinoma samples.

Under this criterion, one or more loci in the *p15/p14ARF/p16* gene region were judged as homozygously deleted in 8 of 28 primary tumors and in 5 of 22 brain metastases (Table 1). Representative adenocarcinoma cases judged as having HDs of this region by MLPA analysis are shown in Fig. 1C. Case B-2P showed a HD of only one locus (probe no. 13) in exon 2 of the *p16* gene. On the other hand, most of the other 12 cases showed HDs of several genes, including the *p14ARF* and/or *p16* genes (Table 2). Both the invasive region (C-10P-in) and the BAC component (C-10P-BAC) of case C-10P showed HDs of the same loci from *p15* exon 1 to *IFNW1*. In case D-4P, the *p15*, *p14ARF*, *p16*, and *MTAP* genes were homozygously deleted. A metastasis to the brain, case N2131M, showed a large HD of the region from the *ELAVL2* gene to the *IFNB1* gene including the *p16* gene. Furthermore, the relative DNA copy number ratios of the corresponding loci were also decreased in the corresponding primary tumor, N2133P, although the ratios were underrepresented as HDs. This may be attributed to a

Table 2. Regions of p16 HDs on chromosome 9p defined by MLPA analysis

No.	Case		Probe no.																						
	Primary tumor	Brain metastasis	1	2	3	4	5	6	7	8	9	10	11	12	13	14	15	16	17	18	19	20	21	22	23	24
1	B-2P		-	-	-	-	-	-	-	-	-	-	-	-	+	-	-	-	-	-	-	-	-	-	-	-
2	B-8P		-	+	-	+	+	+	-	+	+	-	+	+	+	+	+	+	-	-	-	-	-	-	-	-
3	C-5P		-	-	+	+	+	+	+	+	+	+	+	+	+	+	+	+	+	+	+	+	+	+	+	-
4	C-8P		-	+	+	+	+	+	+	+	+	+	+	+	+	+	+	+	+	+	+	+	+	+	+	-
5	C-10P		-	-	+	+	+	+	+	+	+	+	+	+	+	+	+	+	+	+	+	+	-	-	-	-
6	C-65P		-	-	+	+	+	+	+	+	+	-	+	+	+	+	+	+	+	+	+	-	-	-	-	-
7	D-4P		-	-	+	+	+	+	+	+	+	+	+	+	+	+	+	+	-	-	-	-	-	-	-	-
8	D-12P		-	+	+	+	+	+	+	+	+	+	+	+	+	+	+	+	+	+	+	+	+	-	-	-
9		N181M	-	-	+	+	+	+	+	+	+	+	+	+	+	+	+	+	-	-	-	-	-	-	-	-
10		N571M	-	-	+	+	+	+	+	+	+	+	+	+	+	+	+	+	-	-	-	-	-	-	-	-
11	N2133P	N2131M	-	+	+	+	+	+	+	+	+	+	+	+	+	+	+	+	+	+	+	+	+	-	-	-
12		N2151M	-	-	+	+	+	+	+	+	+	+	+	+	+	+	+	+	+	+	+	+	+	+	-	-
13		N2191M	-	+	+	+	+	+	+	+	-	-	-	-	-	-	-	-	-	-	-	-	-	-	-	-

NOTE: Loci with copy number ratios <0.37 are indicated by (+) and those >0.37 are indicated by (-).

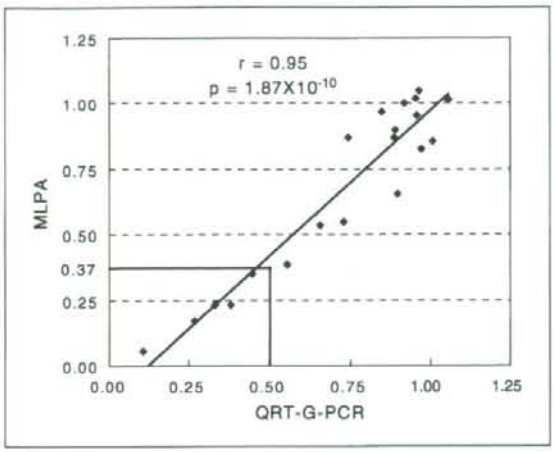

Fig. 2. Correlation between the results of MLPA analysis and those of QRT-G-PCR analysis. Relative DNA copy numbers of the probe no. 9 locus in Fig. 1A on chromosome 9 against the control locus on chromosome 2 defined by the QRT-G-PCR (*X*-axis) and MLPA analyses (*Y*-axis). Sixteen brain metastases and four of the corresponding primary tumors were analyzed. Values <0.5 by QRT-G-PCR analysis and values <0.37 by MLPA analysis (indicated by lines) were considered as having HDs.

contamination of noncancerous cells in the primary tumor sample because this sample was macrodissected but not microdissected. There was no probe loci deleted in all the cases, but six loci (probe nos. 4, 5, 6, 8, 9, and 13) were deleted in 12 of 13 cases, including exon 2 of the *p16* gene (Table 2).

Confirmation of HDs by QRT-G-PCR analysis. QRT-G-PCR was performed to confirm p16 HDs detected by MLPA analysis. Among 15 control probes for nonchromosome 9p loci, a probe for a chromosome 2p14 locus showed the most consistent DNA copy number ratios of nearly 1.0 in surgically resected adenocarcinoma samples. Thus, two primer sets were designed for QRT-G-PCR analysis. One was for the amplification of an MLPA probe locus between the *p14ARF* gene and the *p16* gene (probe no. 9 in Fig. 1A, and hereinafter referred to as the *p14ARF/p16* locus), and the other was for the amplification of a control probe locus on chromosome 2p14.

QRT-G-PCR was carried out for 16 brain metastases and the corresponding 4 primary tumors. Among them, five brain metastases were judged as having HDs of the *p14ARF/p16* locus by MLPA analysis. DNA from normal lung tissue was used as a negative control, and DNA from two lung cancer cell lines with p16 HDs, A549 and H2126, were used as positive controls. No PCR products were detected for the *p14ARF/p16* locus in the A549 and H2126 cell lines (data not shown). The DNA copy number ratios of the *p14ARF/p16* locus in all five cases that had been determined to have HDs of this locus by MLPA analysis were <0.45. Thus, these five cases were also judged as having less than one copy of the *p14ARF/p16* gene by QRT-G-PCR analysis. We further analyzed the association between the results of MLPA analysis and those of QRT-G-PCR analysis among all the 20 cases. The correlation coefficient was 0.95, and a highly significant correlation was observed between them ($P = 1.87 \times 10^{-10}$; Fig. 2). This result gave the agreement for the appropriateness of the criterion for p16 HDs in MLPA analysis.

Occurrence of p16 HDs in early stage lung adenocarcinoma. Based on the results of MLPA analysis, together with the confirmation by QRT-G-PCR analysis, we concluded that p16 HDs were present in 8 of 28 (29%) small-sized primary tumors and in 5 of 22 (23%) brain metastases (Table 1). Among four pairs of brain metastases and the corresponding primary tumors, only one metastasis (N2131M) was judged as having a p16 HD as described above and shown in Fig. 1C, and none of the remaining three cases showed HD in either brain metastases or primary tumors. Small-sized adenocarcinomas

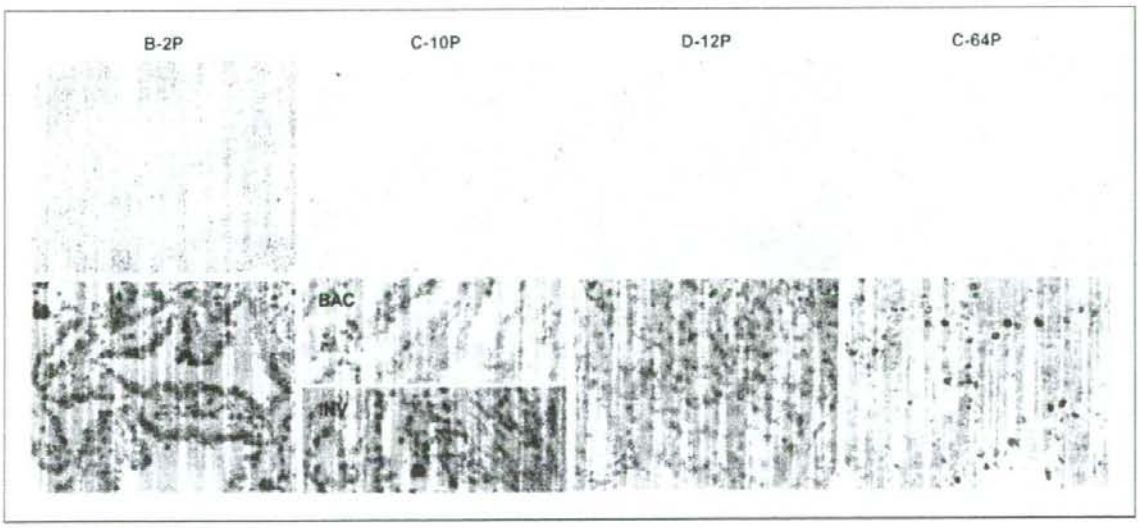

Fig. 3. Histology (H&E; original magnification, ×100 for B-2P/C-12P/C-64P and ×40 for C-10P; *top*) of small-sized lung adenocarcinomas and immunohistochemical staining of p16 protein (original magnification, ×400; *bottom*) in the corresponding tissues. B-2P, C-10P, and D-12P are representative cases of type B, C, and D tumors with p16-negative staining, and C-64P is a representative case of type C tumors with p16-positive staining. A BAC component (*BAC*) and an invasive region (*INV*) are shown separately for C-10P.

Table 3. Associations of p16 HDs with p16 protein expression, clinicopathologic characteristics, and EGFR/KRAS/p53 mutations in lung adenocarcinoma

Clinicopathologic characteristic and genotype	Subset	No. of cases	p16 HD (%)		P*
			+	-	
p16 protein expression †	+	13	0 (0)	13 (100)	<0.01
	-	15	8 (53)	7 (47)	
Gender	Male	30	7 (23)	23 (77)	0.74
	Female	20	6 (30)	14 (70)	
Age	<59	25	8 (32)	17 (68)	0.52
	≥59	25	5 (20)	20 (80)	
Smoking history	Smoker	28	7 (25)	21 (75)	>0.99
	Nonsmoker	22	6 (27)	16 (73)	
Pathologic stage †	I	16	5 (31)	11 (69)	>0.99
	II-III	12	3 (25)	9 (75)	
5-year survival †	+	19	4 (21)	15 (79)	0.37
	-	9	4 (44)	5 (56)	
EGFR/KRAS ‡	E(+)/K(-)	34	10 (29)	24 (71)	]>0.99
	E(-)/K(+)	4	1 (25)	3 (75)	]>0.99] 0.47
	E(-)/K(-)	12	2 (17)	10 (83)	
p53	Mutation(+)	32	9 (28)	23 (72)	0.75
	Mutation(-)	18	4 (22)	14 (78)	

*Fisher's exact test.
† Defined for 28 patients with primary lung adenocarcinoma.
‡ E(+), EGFR mutation(+); E(-), EGFR mutation(-); K(+), KRAS mutation(+); K(-), KRAS mutation(-).

were further classified histologically into types B, C, and D (Fig. 3). Type B tumors are noninvasive BACs and type C tumors are invasive adenocarcinomas with noninvasive BAC components. p16 HDs were detected in 2 of 8 (25%) type B tumors and in 4 of 15 (27%) type C tumors, in particular, in BAC components of two type C tumors (cases C-10P and C-65P). Type D tumors are invasive, poorly differentiated adenocarcinomas and p16 HDs were detected in 2 of 5 (40%) of the type D tumors. Thus, p16 HDs were present with similar frequencies of 25% to 40% in noninvasive and invasive primary adenocarcinomas. We previously reported that p16 HDs were present in 20 of 55 (36%) lung adenocarcinoma cell lines (17). Thus, the frequency of p16 HDs in small-sized primary adenocarcinomas was not significantly lower than, but similar to, those in brain metastases and cultured cell lines. These results strongly indicate that most p16 HDs detected in the cell lines occurred *in vivo* during adenocarcinoma progression and were retained during cultivation *in vitro* of adenocarcinoma cell lines. Similar frequencies of p16 HDs between noninvasive and invasive adenocarcinomas and between primary and metastatic adenocarcinomas further indicate that p16 HD occurs early in the multistage carcinogenic process of lung adenocarcinomas.

No p16 expression in tumors with p16 HDs. Because one of the purposes of this study was to confirm the immunohistochemical negativity of adenocarcinoma cells with p16 HDs, we further performed an immunohistochemical analysis on 28 cases of small-sized adenocarcinomas, all of which were subjected to MLPA analysis. Fifteen of the 28 cases (54%) showed negative immunoreactivity for p16 protein. As predicted, all eight cases with p16 HDs following MLPA analysis were negative for p16 protein expression (Table 3). Representative results of immunohistochemical staining for type B, C, and D tumors are shown in Fig. 3. It was noted that most tumor cells were clearly negative for nuclear p16 staining in these eight cases, and that both BAC components and invasive regions were negative in all four type C tumors with p16 HDs. This result strongly supports the reliability of MLPA analysis for the detection of p16 HDs in primary lung adenocarcinomas. Thus, it was concluded that p16 protein is not expressed in a considerable fraction of small-sized lung adenocarcinomas due to HDs of the p16 gene. The consistency of the results of immunohistochemistry with that of MLPA analysis further supports the hypothesis that *p16* HD occurs early in lung adenocarcinoma progression.

Previously, Dr. Noguchi, who is one of the authors of this article, and his colleagues reported that 29 of 57 (51%) small-sized lung adenocarcinomas of types A to F were negative for p16 immunostaining (7). In their report, the frequency of p16 negativity was higher in smokers and in patients with non-BACs. Aberrant methylation of the *p16* gene promoter was detected more frequently in advanced BACs (type C) and non-BAC (types D–F) than in BACs (types A and B). In this study, the overall frequency (54%) of p16 negativity was quite similar to their reports, and the frequency was also higher in smokers than in nonsmokers (9 of 13 versus 6 of 15), and in type D (5 of 5) than in type B (7 of 15) or type C (3 of 8). Thus, it was highly suggested that a majority of cases with negative p16 expression without p16 HDs could be due to methylation of the *p16* gene promoter and the methylation was associated with tobacco smoking. However, methylation and HD are not likely to coexist with each other because the regions of HDs in most of the 13 cases with HDs included the promoter region of the *p16* gene (from probe no. 8 to probe no. 11). Thus, either methylation or HD of the *p16* gene was suggested to occur equally and independently in smokers, whereas HD dominates in nonsmokers.

Association of p16 HDs with clinicopathologic characteristics. We then investigated the association of p16 HDs with clinicopathologic characteristics, including smoking history, of

patients with lung adenocarcinomas (Table 3). No significant associations were observed between p16 HDs and gender, age, and smoking history in all 50 cases analyzed (Table 3), as well as in 28 cases of primary adenocarcinomas or in 22 cases of brain metastases (data not shown). p16 HDs were not associated with pathologic stage nor with 5-year survival in 28 cases of primary adenocarcinomas (Table 3). Previously, p16 methylation was shown to be associated with smoking history (1, 7). Thus, no association of p16 HDs with smoking history was in contrast with the status of p16 methylation in lung adenocarcinomas. The results indicate that causative factors for p16 HD were different from those for p16 methylation, although both alterations result in the inactivation of the same gene. Previously, Kraunz and colleagues reported that p16 HD occurred at a higher frequency in never-smokers as compared with former and current smokers (6). Although such an association was not observed in this study, both studies indicated the absence of a positive association between p16 HD and smoking history, and the possible association of p16 HD with other causative factors for lung adenocarcinoma. Thus, further studies are needed for the elucidation of such factors because little is known about the environmental as well as genetic risk factors for lung adenocarcinoma. The absence of any association between p16 HDs and 5-year survival was also in contrast with the status of p16 methylation in lung adenocarcinomas. However, because the number of cases examined was small (28 cases), and the patients with poor prognosis had a higher frequency of p16 HDs than those with good prognosis (44% versus 21%), further studies will be required on this subject. The absence of any association between p16 HDs and pathologic stage further supports their occurrence in the early stages, rather than in the late stages, of lung adenocarcinoma progression.

Association of p16 HDs with EGFR, KRAS, and p53 mutations. We next evaluated the association of p16 HDs with the status of EGFR, KRAS, and p53 mutations in these samples (Tables 1 and 3). Then, based on the results of these molecular analyses and a previous p16 methylation analysis (7), a stepwise malignant progression model for small-sized lung adenocarcinoma was depicted as shown in Fig. 4. As previously reported (14, 18), EGFR and KRAS mutations were detected in a mutually exclusive manner in lung adenocarcinomas. EGFR mutations were most frequently detected in type B tumors (8 of 8, 100%), suggesting the involvement of EGFR mutations in the formation of noninvasive BACs. Although KRAS mutations were detected only in type C and D tumors in this study, it was recently reported that the mutations were frequently detected in noninvasive adenocarcinomas and also in atypical adenomatous hyperplasias (AAH; ref. 19). Thus, it is likely that either EGFR or KRAS mutations occur prior to HDs and methylations of the p16 gene in the progression of BACs, although it is also possible that p16 alterations occur earlier than depicted in Fig. 4. Frequencies of p53 mutations in primary adenocarcinomas were the highest in type D (5 of 5, 100%), intermediate in type C (9 of 15, 60%), and the lowest in type B (2 of 8, 25%), suggesting the accumulation of the mutations during progression from noninvasive adenocarcinomas to invasive ones. Thus, it was likely that p53 mutations had accumulated in adenocarcinomas with p16 HDs and/or EGFR/KRAS mutations. It is indispensable to analyze a considerable number of AAHs as well as type A tumors to fully understand the timing of each genetic alteration in sequential progression of lung adenocarcinomas because AAH is a putative precursor of peripheral lung adenocarcinoma including BAC (20), and sequential progression from type A to type C tumors through type B tumors was strongly indicated in previous

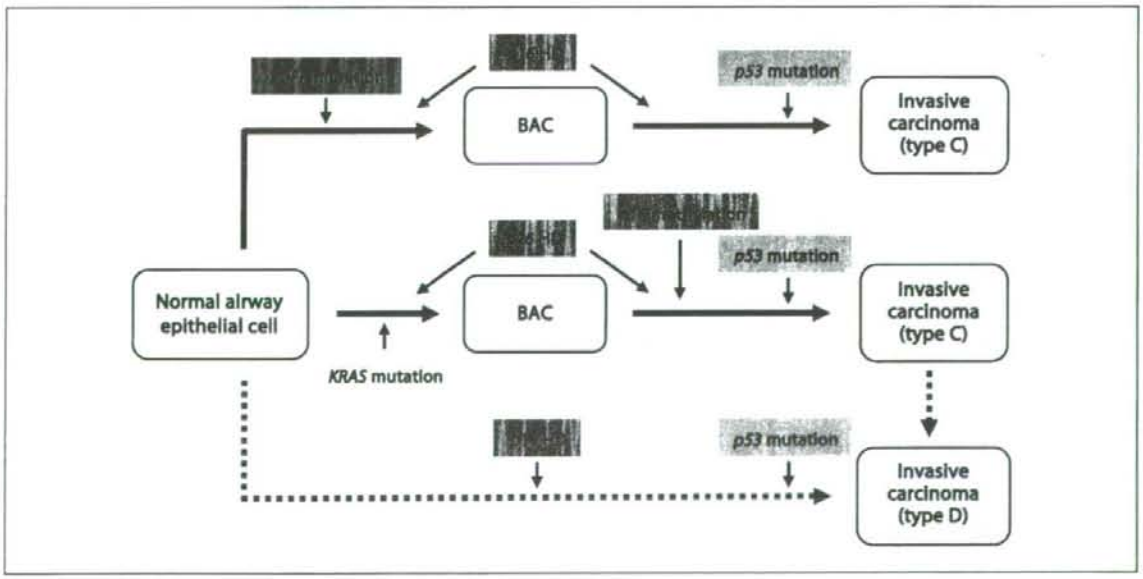

Fig. 4. A stepwise malignant progression model of small-sized lung adenocarcinoma in association with accumulated genetic alterations in cells. BAC, bronchioloalveolar carcinoma; type C, localized bronchioloalveolar carcinoma with foci of active fibroblastic proliferation; type D, poorly differentiated adenocarcinoma.

studies (7, 21). However, because AAH is not routinely resected by surgery and because type A tumors are usually very small, the number of tumors as well as the amount of DNA obtained was not enough for the present study.

There was no specificity for the occurrence of p16 HDs among adenocarcinomas with regard to other accompanied genetic alterations. In particular, p16 HDs were detected with similar frequencies (17–29%), irrespective of the presence or absence of EGFR, KRAS, and p53 mutations (Table 3). This result indicates that p16 HDs occur with similar frequencies in EGFR type as well as KRAS type and non-EGFR/KRAS type adenocarcinomas. In this model, type C tumors were considered to progress from BACs, as previously indicated by Aoyagi and colleagues (21). However, it was still unclear whether type D tumors arise *de novo* by a distinct pathway from tumors with BAC components or progress from these tumors. Low frequencies of EGFR mutations and high frequencies of p53 mutations in type D tumors indicate that type D tumors progress from either the KRAS types or non-EGFR/KRAS types. Haneda and colleagues also reported a low frequency of EGFR mutations in type D tumors (22), supporting the presence of a non-EGFR pathway for the development of type D poorly differentiated adenocarcinomas.

Conclusions. MLPA analysis of microdissected small-sized primary adenocarcinoma cells revealed that p16 HDs are present in 20% to 40% of adenocarcinomas irrespective of the presence of mutations in the *EGFR*, *KRAS*, and *p53* genes, and occur early in the development of lung adenocarcinomas. HDs were not associated with smoking history of the patients. It has been indicated that smoking is a major factor inducing p16 methylation as well as KRAS mutation. In contrast, EGFR mutations frequently occur in female nonsmokers and are associated with bronchioloalveolar morphology of adenocarcinomas. Interestingly, p16 HDs did not coexist with specific genetic alterations in adenocarcinoma cells. Thus, causative factors for p16 HD would be different from those for p16 methylation, KRAS mutations, and EGFR mutations. To elucidate the causative role for the occurrence of p16 HDs in multistage lung carcinogenesis, further studies should focus on the identification of environmental and genetic factors for the induction of DNA double-strand breaks surrounding the *p16* gene locus and their repair systems.

Disclosure of Potential Conflicts of Interest

No potential conflicts of interest were disclosed.

Acknowledgments

We thank Drs. Higashi and Yokoyama of FALCO Biosystems, Ltd., for their technical support and critical discussion in MLPA analysis. We also thank Drs. Nakanishi and Matsumoto for the laser capture microdissection of cancer cells from primary small-sized lung adenocarcinomas.

References

1. Toyooka S, Tokumo M, Shigematsu H, et al. Mutational and epigenetic evidence for independent pathways for lung adenocarcinomas arising in smokers and never smokers. Cancer Res 2006;66:1371–5.
2. Sato M, Shames DS, Gazdar AF, Minna JD. A translational view of the molecular pathogenesis of lung cancer. J Thorac Oncol 2007;2:327–43.
3. Hamada K, Kohno T, Kawanishi M, Ohwada S, Yokota J. Association of CDKN2A(p16)/CDKN2B(p15) alterations and homozygous chromosome arm 9p deletions in human lung carcinoma. Genes Chromosomes Cancer 1998;22:232–40.
4. Sanchez-Cespedes M, Reed AL, Buta M, et al. Inactivation of the INK4A/ARF locus frequently coexists with TP53 mutations in non-small cell lung cancer. Oncogene 1999;18:5843–9.
5. Sanchez-Cespedes M, Decker PA, Doffek KM, et al. Increased loss of chromosome 9p21 but not p16 inactivation in primary non-small cell lung cancer from smokers. Cancer Res 2001;61:2092–6.
6. Krausz KS, Nelson HH, Lemos M, Godleski JJ, Wiencke JK, Kelsey KT. Homozygous deletion of p16INK4a and tobacco carcinogen exposure in non-small cell lung cancer. Int J Cancer 2006;118:1364–9.
7. Tanaka R, Wang D, Morishita Y, et al. Loss of function of p16 gene and prognosis of pulmonary adenocarcinoma. Cancer 2005;103:608–15.
8. Chen JT, Chen YC, Wang YC, Tseng RC, Chen CY, Wang YC. Alterations of the p16(ink4a) gene in resected nonsmall cell lung tumors and exfoliated cells within sputum. Int J Cancer 2002;98:724–31.
9. Schouten JP, McElgunn CJ, Waaijer R, Zwijnenburg D, Diepvens F, Pals G. Relative quantification of 40 nucleic acid sequences by multiplex ligation-dependent probe amplification. Nucleic Acids Res 2002;30:e57.
10. Worsham MJ, Chen KM, Tiwari N, et al. Fine-mapping loss of gene architecture at the CDKN2B (p15INK4b), CDKN2A (p14ARF, p16INK4a), and MTAP genes in head and neck squamous cell carcinoma. Arch Otolaryngol Head Neck Surg 2006;132:409–15.
11. Mistry SH, Taylor C, Randerson-Moor JA, et al. Prevalence of 9p21 deletions in UK melanoma families. Genes Chromosomes Cancer 2005;44:292–300.
12. Sobin LH, Wittekind CH, editors. TNM classification of malignant tumours. 6th ed. New York: Wiley-Liss; 2002. p. 99–103.
13. Noguchi M, Morikawa A, Kawasaki M, et al. Small adenocarcinoma of the lung. Histologic characteristics and prognosis. Cancer 1995;75:2844–52.
14. Matsumoto S, Iwakawa R, Kohno T, et al. Frequent EGFR mutations in noninvasive bronchioloalveolar carcinoma. Int J Cancer 2006;118:2498–504.
15. Sakamoto H, Mori M, Taira M, et al. Transforming gene from human stomach cancers and a noncancerous portion of stomach mucosa. Proc Natl Acad Sci U S A 1986;83:3997–4001.
16. Matsumoto S, Takahashi K, Iwakawa R, et al. Frequent EGFR mutations in brain metastases of lung adenocarcinoma. Int J Cancer 2006;119:1491–4.
17. Hamada K, Kohno T, Takahashi M, et al. Two regions of homozygous deletion clusters at chromosome band 9p21 in human lung cancer. Genes Chromosomes Cancer 2000;27:308–18.
18. Riely GJ, Politi KA, Miller VA, Pao W. Update on epidermal growth factor receptor mutations in non-small cell lung cancer. Clin Cancer Res 2006;12:7232–41.
19. Sakamoto H, Shimizu J, Horio Y, et al. Disproportionate representation of KRAS gene mutation in atypical adenomatous hyperplasia, but even distribution of EGFR gene mutation from preinvasive to invasive adenocarcinomas. J Pathol 2007;212:287–94.
20. Travis WD, Brambilla E, Muller-Hermelink HK, Harris CC, editors. Pathology and genetics: tumours of the lung, pleura, thymus and heart. Lyon: IARC Press; 2004. p. 73–5.
21. Aoyagi Y, Yokose T, Minami Y, et al. Accumulation of losses of heterozygosity and multistep carcinogenesis in pulmonary adenocarcinoma. Cancer Res 2001;61:7950–4.
22. Haneda H, Sasaki H, Shimizu S, et al. Epidermal growth factor receptor gene mutation defines distinct subsets among small adenocarcinomas of the lung. Lung Cancer 2006;52:47–52.

Biochemical and Biophysical Research Communications 374 (2008) 394–398

Contents lists available at ScienceDirect

Biochemical and Biophysical Research Communications

journal homepage: www.elsevier.com/locate/ybbrc

Podocalyxin expression in malignant astrocytic tumors

Norihito Hayatsu [a], Mika Kato Kaneko [b], Kazuhiko Mishima [c], Ryo Nishikawa [c], Masao Matsutani [c], Janet E. Price [b], Yukinari Kato [b,*]

[a] Graduate School of Medicine, Kyoto University, Yoshida-konoe-cho, Sakyo-ku, Kyoto 606-8501, Japan
[b] Department of Cancer Biology, Unit 173, University of Texas M.D. Anderson Cancer Center, 1515 Holcombe, Houston, TX 77030, USA
[c] Saitama Medical University International Medical Center, 1397-1 Yamane Hidaka-shi, Saitama 350-1298, Japan

ARTICLE INFO

Article history:
Received 4 July 2008
Available online 17 July 2008

Keywords:
Podocalyxin
Keratan sulfate
Proteoglycan
Astrocytic tumor
Glioblastoma

ABSTRACT

Podocalyxin is an anti-adhesive mucin-like transmembrane sialoglycoprotein that has been implicated in the development of aggressive forms of cancer. Podocalyxin is also known as keratan sulfate (KS) proteoglycan. Recently, we revealed that highly sulfated KS or another mucin-like transmembrane sialoglycoprotein podoplanin/aggrus is upregulated in malignant astrocytic tumors. The aim of this study is to examine the relationship between podocalyxin expression and malignant progression of astrocytic tumors. In this study, 51 astrocytic tumors were investigated for podocalyxin expression using immunohistochemistry, Western blot analysis, and quantitative real-time PCR. Immunohistochemistry detected podocalyxin on the surface of tumor cells in six of 14 anaplastic astrocytomas (42.9%) and in 17 of 31 glioblastomas (54.8%), especially around proliferating endothelial cells. In diffuse astrocytoma, podocalyxin expression was observed only in vascular endothelial cells. Podocalyxin might be associated with the malignant progression of astrocytic tumors, and be a useful prognostic marker for astrocytic tumors.

Astrocytic tumors are the most common tumors of the central nervous system (CNS) and are categorized into diffuse astrocytomas (World Health Organization (WHO) Grade II), anaplastic astrocytomas (WHO Grade III), and glioblastomas (WHO Grade IV) [1]. Glioblastoma may occur de novo or may result from progression of low-grade astrocytomas [2]. Molecular mechanisms of malignant progression are associated with inactivation of tumor suppressor genes such as p53-Rb pathway or overexpression of oncogenes such as epidermal growth factor receptor (EGFR) [3]. However, the mechanisms of malignant progression of astrocytic tumors have not been resolved completely. Identification of genes that are expressed differentially in high-grade or low-grade astrocytomas is important to elucidate the molecular mechanisms of malignant progression and to develop novel therapeutic strategies.

Podocalyxin is a type I transmembrane sialoglycoprotein, which belongs to the CD34 family. Podocalyxin is expressed on the surface of various normal cells, including kidney podocytes, vascular endothelial cells, hematopoietic stem cells, and platelets [4–7]. The physiological function of podocalyxin is as an anti-adhesion molecule that maintains open filtration pathways between neighboring podocyte foot processes through the charge-repulsive effects of its large, highly sialylated and sulfated extracellular domain [8]. In canine kidney (MDCK) cells, podocalyxin overexpression leads to the inhibition of cell–cell interaction as shown by decreased cell–cell adhesion, decreased tight junction-dependent transepithelial resistance, and redistribution of cell junction proteins [9]. Decreased cell–cell interaction is a prominent feature of cancer cells that display a metastatic phenotype, suggesting a possible role for anti-adhesive molecules, such as podocalyxin, in cancer progression. The role of podocalyxin in cancer remains unclear, although its expression has been reported in breast, liver, pancreas, kidney, prostate, testis, and blood cell cancers [10–16]. However, podocalyxin has been implicated in the development of aggressive forms of cancer. Increased podocalyxin protein expression is correlated with poor outcome in breast carcinomas, and is implicated in more aggressive forms of prostate cancer [10,14]. Furthermore, podocalyxin variants were found to be associated with both the risk of prostate cancer and prostate tumor aggressiveness. Recently, podocalyxin was reported to increase the aggressive phenotype of breast and prostate cancer in vitro through its interaction with ezrin [17]. Thus, podocalyxin is a candidate for playing a critical role in cancer aggressiveness and malignancy. Podocalyxin is also reported to be useful to differentiate pancreatic ductal adenocarcinomas from adenocarcinomas of the biliary and gastrointestinal tracts [12].

Recently, we showed that the expression of highly sulfated keratan sulfate (KS) recognized by 5D4 antibody is increased in

Abbreviations: KS, keratan sulfate; CNS, central nervous system; WHO, World Health Organization.

* Corresponding author. Fax: +81 29 861 3191.
E-mail address: yukinari-k@bea.hi-ho.ne.jp (Y. Kato).

0006-291X/$ - see front matter © 2008 Elsevier Inc. All rights reserved.
doi:10.1016/j.bbrc.2008.07.049

parallel with increasing malignancy of astrocytic tumors [18,19]. KS expression is induced by high expression of five glycogenes involved in KS synthesis. However, in addition to high expression levels of glycogenes involved in KS synthesis, core proteins of KS proteoglycan also might contribute to the high expression of KS. Podocalyxin was recently identified as a KS proteoglycan [20]. In this study, 51 astrocytic tumors (six diffuse astrocytomas, 14 anaplastic astrocytomas, and 31 glioblastomas) were investigated using immunohistochemistry and Western blot with an anti-podocalyxin antibody. Furthermore, we investigated the podocalyxin transcript levels using quantitative real-time PCR in 51 frozen astrocytic tumors.

Materials and methods

Tissue samples. Tumor specimens were obtained during surgery from six patients with diffuse astrocytomas, 14 patients with anaplastic astrocytomas, and 31 patients with glioblastomas [19,21]. Informed consent had been obtained previously from patients or their guardians. The histology of these tissue samples was confirmed by experienced neuropathologists.

Immunohistochemical analysis. Specimens were deparaffinized, rehydrated and incubated first with goat anti-human podocalyxin (2 μg/ml) at 4 °C for 18 h, then with biotin-conjugated secondary anti-goat IgG antibody (Dako, Glostrup, Denmark) for 1 h, and finally with peroxidase-conjugated biotin-streptavidin complex (Vectastain ABC Kit; Vector Laboratories Inc., Burlingame, CA) for 1 h. Color was developed using 3, 3-diaminobenzidine tetrahydrochloride tablet sets (Dako) for 3 min. KS expression was assessed semi-quantitatively from the percentage of tumor cells with cytoplasmic/membrane staining: 0, no staining; +, <10%; ++, 10–50%; and +++, >50%.

Western blot analysis. The tissues were lysed with lysis buffer (25 mM Tris (pH 7.4), 50 mM NaCl, 0.5% Na deoxycholate, 2% Nonidet P-40, 0.2% SDS, 1 mM phenylmethylsulfonyl fluoride, and 50 mg/ml aprotinin) [19,21]. Samples of the supernatant fraction were collected after centrifuging at 15,000g for 30 min. Four micrograms of the proteins were electrophoresed under reducing conditions on 10% polyacrylamide gel (Atto Bioscience, Tokyo, Japan). The separated proteins were transferred to a PVDF membrane. After blocking with 3% skim milk in PBS with 0.05% Tween 20, the membrane was incubated with goat anti-human podocalyxin (0.1 μg/ml; R&D Systems, Minneapolis, MN) or anti-β-actin antibody (1/5000 dilution; Sigma, St. Louis, MO), and subsequently with peroxidase-conjugated anti-goat or anti-mouse antibodies (1/5000 dilution; Bio-Rad Laboratories Inc., Hercules, CA). It was then developed for 1 min with ECL reagents (Amersham Pharmacia Biotech Inc.) using Amersham Hyperfilm ECL (Amersham Pharmacia Biotech Inc.).

Quantitative real-time PCR analysis. Total RNAs were prepared from 51 astrocytic tumors (six diffuse astrocytomas, 14 anaplastic astrocytomas, and 31 glioblastomas) using an RNeasy mini prep kit (Qiagen Inc., Hilden, Germany). The initial cDNA strand was synthesized using SuperScript III transcriptase (Invitrogen Corp., Carlsbad, CA) by priming an oligo-dT primer according to the manufacturer's instructions. We performed PCR using oligonucleotides: human podocalyxin sense (5′-acaggaaacaccctctgtgc-3′) and human podocalyxin antisense (5′-gaaggtggctttgactgctc-3′). Real-time PCR was carried out using the QuantiTect SYBR Green PCR (Qiagen Inc.). The PCR conditions were 95 °C for 15 min (1 cycle), followed by 40 cycles of 94 °C for 15 s, 53 °C for 20 s, and 72 °C for 10 s. Subsequently, a melting curve program was applied with continuous fluorescence measurement. A standard curve for podocalyxin templates was generated through serial dilution of PCR products (1×10^8 to 1×10^2 copies/μl). The expression level of podocalyxin was normalized by total RNA weights. The statistical significance of podocalyxin mRNA expression in astrocytic tumor tissues was determined using paired *t* tests.

Statistical analyses. Results are expressed as the mean ± standard deviation. Student's *t*-test was used to determine significance among the groups. A value of $p < 0.05$ was considered significant.

Results

Immunohistochemical staining for podocalyxin in malignant astrocytic tumors

The cellular distribution of podocalyxin in astrocytic tumors was examined immunohistochemically using goat anti-human podocalyxin polyclonal antibody. This polyclonal antibody was produced in goats immunized with recombinant human podocalyxin extracellular domain (23–425 a.a.), and purified using podocalyxin affinity chromatography. In many recent studies, this antibody was applied to the immunohistochemistry, Western blot, and immunoprecipitation, indicating that this antibody is specific to human podocalyxin [20,22,23]. Herein, we used 51 surgical tissue samples (six diffuse astrocytomas: Grade II, 14 anaplastic astrocytomas: Grade III, and 31 glioblastomas: Grade IV) for immunohistochemistry. Podocalyxin immunoreactivity was detected in six of 14 (42.9%) anaplastic astrocytomas and in 17 of 31 (54.8%) glioblastomas; staining was graded as +++ in seven glioblastoma and as ++ in three glioblastoma cases (Table 1). Podocalyxin was not detected on tumor cell surfaces in diffuse astrocytomas, yet was observed in vascular endothelial cells in these specimen (Fig. 1A and B). Representative staining for podocalyxin in astrocytic tumor samples is shown in Fig. 1. Immunostaining for podocalyxin demonstrated predominantly cell-surface patterns. In anaplastic astrocytoma, the tumor cell surface was stained using anti-podocalyxin (Fig. 1C and D). In glioblastomas, podocalyxin-positive tumor cells were prominent around microvascular proliferations (Fig. 1E and F). Proliferating endothelial cells were also positive for podocalyxin (Fig. 1F).

Analysis of podocalyxin expression using Western blot in astrocytic tumors

To confirm the podocalyxin expression in astrocytic tumors, lysates of frozen tumor specimens from 51 patients were analyzed using Western blot analysis with anti-podocalyxin antibody. As shown in Fig. 2, podocalyxin was highly detected in extracts of anaplastic astrocytoma and glioblastoma. Samples of one of 14 anaplastic astrocytomas (7.1%) and seven of 31 glioblastomas (22.6%) showed relatively high levels of podocalyxin, while expression in five of 14 anaplastic astrocytomas (35.7%) and 11 of 31 glioblastomas (35.5%) was more moderate. The other astrocytic tumors including diffuse astrocytic tumors produced weak immunoreactive bands, since podocalyxin is expressed in all vascular endothelial cells (Fig. 1).

Table 1
Results of podocalyxin immunostaining in 51 patients with astrocytic tumors

Tumor type	No. of cases	Podocalyxin				Positive rate
		+++	++	+	–	
Diffuse astrocytoma (grade II)	6	0	0	0	6	0%
Anaplastic astrocytoma (grade III)	14	0	1	5	8	42.9%
Glioblastoma (grade IV)	31	7	3	7	14	54.8%

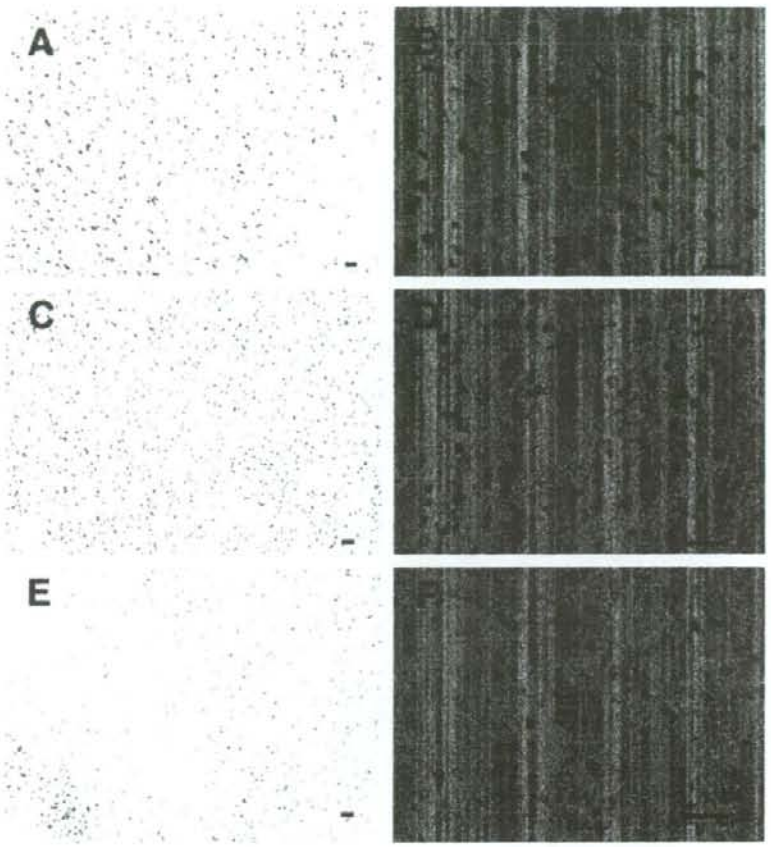

Fig. 1. Immunohistochemical detection of podocalyxin in astrocytic tumors. Podocalyxin was not detected on tumor cell surfaces in diffuse astrocytomas; however, podocalyxin staining was observed in vascular endothelial cells, although as shown in this figure few endothelial cells are usually detected in diffuse astrocytomas (A: 100×, B: 400×). In anaplastic astrocytoma, the tumor cell surface was stained positively (C: 100×, D: 400×). Accentuated staining is visible around an area of microvascular proliferation in glioblastoma (E: 100×, F: 400×). Bar, 10 μm.

Differential expression of the podocalyxin mRNA in astrocytic tumors

To quantify the expression of podocalyxin mRNA in human astrocytic tumors of different grades, we performed quantitative real-time PCR analyses of astrocytic tumors from 51 patients. The relative podocalyxin mRNA expression levels of each tumor grade are shown in Fig. 3. Average copy numbers of podocalyxin mRNA/μg total RNA in diffuse astrocytomas, anaplastic astrocytomas, and glioblastomas were 535 ± 289, 918 ± 595, and 3670 ± 2916, respectively. Podocalyxin transcript levels were significantly higher in glioblastomas than in diffuse astrocytomas or anaplastic astrocytomas ($p < 0.01$).

Discussion

Podocalyxin expression has been reported to increase the aggressive phenotype of breast and prostate cancer, and be correlated with their poor prognosis [10,14,17]. Recently, we showed that highly sulfated keratan sulfate detected by 5D4 antibody is upregulated in accordance with malignancy of astrocytic tumors [19]. We speculated that expression of core proteins of KS proteoglycan is upregulated in malignant astrocytic tumors. Podocalyxin was recently identified as a keratan sulfate (KS) proteoglycan: podocalyxin has the keratan sulfate antigens TRA-1-60 and TRA-1-81, which are also known as human pluripotent stem cell markers, in embryonal carcinoma [20]. Furthermore, podocalyxin expression correlates with tumor aggressiveness or malignancy; therefore, we herein investigated the podocalyxin expression in brain tumors, focusing on astrocytic tumors of different grades.

In this study, we first investigated the podocalyxin expression by immunohistochemistry (Fig. 1), and showed significantly different podocalyxin expression between anaplastic astrocytomas (Grade III; 42.9%) and glioblastoma (Grade IV; 54.8%; $p < 0.05$). Using Western blot analysis and real-time PCR, we confirmed this result (Figs. 2 and 3). Taken together, these results indicate that podocalyxin expression might be associated with the malignant progression of astrocytic tumors. We previously investigated the expression of podoplanin, another mucin-like sialoglycoprotein, which is associated with malignant progression of astrocytic tumors [21,24,25]. Podoplanin was detected on the cell surface in 27% of anaplastic astrocytomas and 47% of glioblastomas. In contrast, podoplanin expression was not observed in diffuse astrocytomas. Because both podocalyxin and podoplanin are associated with the malignancy of astrocytic tumors, we investigated whether podocalyxin expression is correlated with podoplanin; however, we found no correlation between the expression levels of the two sialoglycoproteins (data not shown). We might be able to predict the malignancy of astrocytic tumors if we appropriately combine

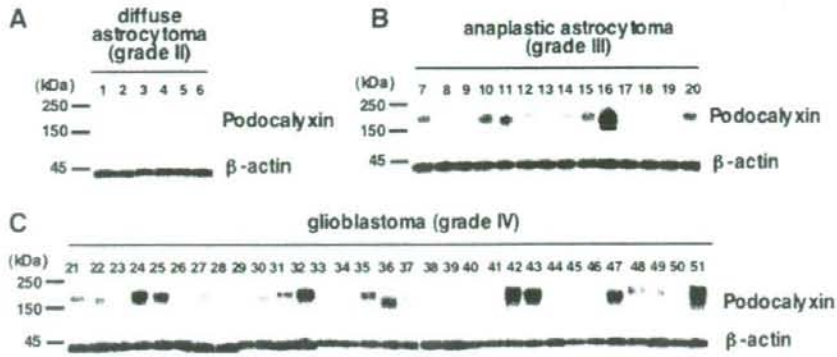

Fig. 2. Western blot analysis of podocalyxin expression in astrocytic tumors. Tissues from diffuse astrocytomas (A: lane 1–6), anaplastic astrocytomas (B: lane 7–20), and glioblastomas (C: lane 21–51) were solubilized, and 4 μg of the proteins were electrophoresed under reducing conditions on 10% polyacrylamide gel. The separated proteins were transferred to a PVDF membrane. After blocking with 3% skim milk in PBS, the membrane was incubated with anti-podocalyxin (upper panel) or anti-β-actin antibody (lower panel).

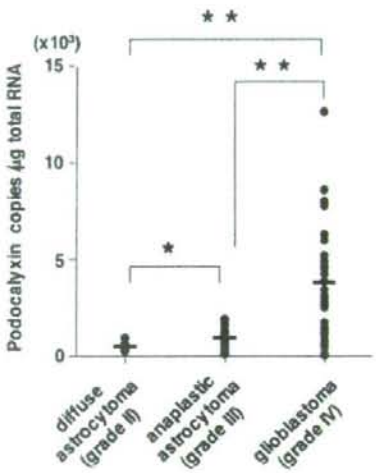

Fig. 3. Quantitative real-time PCR analysis of podocalyxin in astrocytic tumors. The transcript levels for a podocalyxin gene in 51 astrocytic tumors (six diffuse astrocytomas, 14 anaplastic astrocytomas, and 31 glioblastomas) were measured using real-time PCR. Values normalized to the level of total RNA are presented. $^{**}p < 0.01$, $^{*}p < 0.05$.

the expression level of these several molecules. Further study is needed to clarify the pathophysiological function of podocalyxin in astrocytic tumors, such as invasiveness or angiogenesis, using more clinical samples.

In summary, we investigated the expression of podocalyxin in 51 astrocytic tumors using immunohistochemistry, Western blot, and real-time PCR analyses. Podocalyxin expression was not observed in diffuse astrocytoma except in vascular endothelial cells. Furthermore, podocalyxin mRNA and protein expression were markedly higher in glioblastomas than in anaplastic astrocytomas. These data suggest that podocalyxin expression is associated with malignancy of astrocytic tumors, and might be useful as a prognostic factor.

Acknowledgments

This study was supported in part by Mitsubishi Pharma Research Foundation (Y. Kato), the YASUDA Medical Foundation (Y. Kato), the Toyama Foundation (Y. Kato), the Inoue Foundation for Science (Y. Kato), and Osaka Cancer Research Foundation (M.K. Kaneko).

References

[1] P. Kleihues, P.C. Burger, V.P. Collines, E.W. Newcomb, H. Ohagi, W.K. Cavenee, Astrocytic Tumors, Glioblastma, International Agency for Research on Cancer Press, Lyons, France, 2000. pp. 29–39.
[2] A. Giese, R. Bjerkvig, M.E. Berens, M. Westphal, Cost of migration: invasion of malignant gliomas and implications for treatment, J. Clin. Oncol. 21 (2003) 1624–1636.
[3] P. Kleihues, H. Ohgaki, Primary and secondary glioblastomas: from concept to clinical diagnosis, Neuro-oncology 1 (1999) 44–51.
[4] D. Kerjaschki, D.J. Sharkey, M.G. Farquhar, Identification and characterization of podocalyxin-the major sialoprotein of the renal glomerular epithelial cell, J. Cell Biol. 98 (1984) 1591–1596.
[5] J.E. Schnitzer, C.P. Shen, G.E. Palade, Lectin analysis of common glycoproteins detected on the surface of continuous microvascular endothelium in situ and in culture: identification of sialoglycoproteins, Eur. J. Cell Biol. 52 (1990) 241–251.
[6] T. Hara, Y. Nakano, M. Tanaka, K. Tamura, T. Sekiguchi, K. Minehata, N.G. Copeland, N.A. Jenkins, M. Okabe, H. Kogo, Y. Mukouyama, A. Miyajima, Identification of podocalyxin-like protein 1 as a novel cell surface marker for hemangioblasts in the murine aorta-gonad-mesonephros region, Immunity 11 (1999) 567–578.
[7] A. Miettinen, M.L. Solin, J. Reivinen, E. Juvonen, R. Vaisanen, H. Holthofer, Podocalyxin in rat platelets and megakaryocytes, Am. J. Pathol. 154 (1999) 813–822.
[8] R. Doyonnas, D.B. Kershaw, C. Duhme, H. Merkens, S. Chelliah, T. Graf, K.M. McNagny, Anuria, omphalocele, and perinatal lethality in mice lacking the CD34-related protein podocalyxin, J. Exp. Med. 194 (2001) 13–27.
[9] T. Takeda, W.Y. Go, R.A. Orlando, M.G. Farquhar, Expression of podocalyxin inhibits cell–cell adhesion and modifies junctional properties in Madin–Darby canine kidney cells, Mol. Biol. Cell 11 (2000) 3219–3232.
[10] A. Somasiri, J.S. Nielsen, N. Makretsov, M.L. McCoy, L. Prentice, C.B. Gilks, S.K. Chia, K.A. Gelmon, D.B. Kershaw, D.G. Huntsman, K.M. McNagny, C.D. Roskelley, Overexpression of the anti-adhesin podocalyxin is an independent predictor of breast cancer progression, Cancer Res. 64 (2004) 5068–5073.
[11] X. Chen, J. Higgins, S.T. Cheung, R. Li, V. Mason, K. Montgomery, S.T. Fan, M. van de Rijn, S. So, Novel endothelial cell markers in hepatocellular carcinoma, Mod. Pathol. 17 (2004) 1198–1210.
[12] J.T. Ney, H. Zhou, B. Sipos, R. Buttner, X. Chen, G. Kloppel, I. Gutgemann, Podocalyxin-like protein 1 expression is useful to differentiate pancreatic ductal adenocarcinomas from adenocarcinomas of the biliary and gastrointestinal tracts, Hum. Pathol. 38 (2007) 359–364.
[13] P. Stanhope-Baker, P.M. Kessler, W. Li, M.L. Agarwal, B.R. Williams, The Wilms tumor suppressor-1 target gene podocalyxin is transcriptionally repressed by p53, J. Biol. Chem. 279 (2004) 33575–33585.
[14] G. Casey, P.J. Neville, X. Liu, S.J. Plummer, M.S. Cicek, L.M. Krumroy, A.P. Curran, M.R. McGreevy, W.J. Catalona, E.A. Klein, J.S. Witte, Podocalyxin variants and risk of prostate cancer and tumor aggressiveness, Hum. Mol. Genet. 15 (2006) 735–741.
[15] W.M. Schopperle, D.B. Kershaw, W.C. DeWolf, Human embryonal carcinoma tumor antigen, Gp200/GCTM-2, is podocalyxin, Biochem. Biophys. Res. Commun. 300 (2003) 285–290.
[16] T.W. Kelley, D. Huntsman, K.M. McNagny, C.D. Roskelley, E.D. Hsi, Podocalyxin: a marker of blasts in acute leukemia, Am. J. Clin. Pathol. 124 (2005) 134–142.

[17] S. Sizemore, M. Cicek, N. Sizemore, K.P. Ng, G. Casey, Podocalyxin increases the aggressive phenotype of breast and prostate cancer cells in vitro through its interaction with ezrin, Cancer Res. 67 (2007) 6183–6191.
[18] N. Hayatsu, S. Ogasawara, M.K. Kaneko, Y. Kato, H. Narimatsu, Expression of highly sulfated keratan sulfate synthesized in human glioblastoma cells, Biochem. Biophys. Res. Commun. 368 (2008) 217–222.
[19] Y. Kato, N. Hayatsu, M.K. Kaneko, S. Ogasawara, T. Hamano, S. Takahashi, R. Nishikawa, M. Matsutani, K. Mishima, H. Narimatsu, Increased expression of highly sulfated keratan sulfate synthesized in malignant astrocytic tumors, Biochem. Biophys. Res. Commun. 369 (2008) 1041–1046.
[20] W.M. Schopperle, W.C. DeWolf, The TRA-1-60 and TRA-1-81 human pluripotent stem cell markers are expressed on podocalyxin in embryonal carcinoma, Stem Cells 25 (2007) 723–730.
[21] K. Mishima, Y. Kato, M.K. Kaneko, R. Nishikawa, T. Hirose, M. Matsutani, Increased expression of podoplanin in malignant astrocytic tumors as a novel molecular marker of malignant progression, Acta Neuropathol. (Berlin) 111 (2006) 483–488.
[22] J. Achenbach, M. Mengel, I. Tossidou, I. Peters, J. K. Park, M. Haubitz, J. H. Ehrich, H. Haller, M. Schiffer, Parietal epithelia cells in the urine as a marker of disease activity in glomerular diseases, Nephrol. Dial. Transpl., in press.
[23] A.B. Choo, H.L. Tan, S.N. Ang, W.J. Fong, A. Chin, J. Lo, L. Zheng, H. Hentze, R.J. Philp, S.K. Oh, M. Yap, Selection against undifferentiated human embryonic stem cells by a cytotoxic antibody recognizing podocalyxin-like protein-1, Stem Cells 26 (2008) 1454–1463.
[24] Y. Kato, M.K. Kaneko, A. Kunita, H. Ito, A. Kameyama, S. Ogasawara, N. Matsuura, Y. Hasegawa, K. Suzuki-Inoue, O. Inoue, Y. Ozaki, H. Narimatsu, Molecular analysis of the pathophysiological binding of the platelet aggregation-inducing factor podoplanin to the C-type lectin-like receptor CLEC-2, Cancer Sci. 99 (2008) 54–61.
[25] Y. Kato, M.K. Kaneko, A. Kuno, N. Uchiyama, K. Amano, Y. Chiba, Y. Hasegawa, J. Hirabayashi, H. Narimatsu, K. Mishima, M. Osawa, Inhibition of tumor cell-induced platelet aggregation using a novel anti-podoplanin antibody reacting with its platelet-aggregation-stimulating domain, Biochem. Biophys. Res. Commun. 349 (2006) 1301–1307.

Jpn J Clin Oncol 2008;38(10)715–718
doi:10.1093/jjco/hyn095

Clinical Trial Note

A Multicenter Phase I Trial of Interferon-β and Temozolomide Combination Therapy for High-grade Gliomas (INTEGRA Study)

Toshihiko Wakabayashi[1], Takamasa Kayama[2], Ryo Nishikawa[3], Hiroshi Takahashi[4], Toshiki Yoshimine[5], Nobuo Hashimoto[6], Tomokazu Aoki[7], Kaoru Kurisu[8], Atsushi Natsume[1], Masatoshi Ogura[1] and Jun Yoshida[1]

[1]Department of Neurosurgery, Nagoya University School of Medicine, Nagoya, [2]Department of Neurosurgery, Yamagata University School of Medicine, Yamagata, [3]Department of Neurosurgery, Saitama Medical University, Saitama, [4]Department of Neurosurgery, Nippon Medical School, Tokyo, [5]Department of Neurosurgery, Osaka University School of Medicine, Osaka, [6]Department of Neurosurgery, Kyoto University School of Medicine, Kyoto, [7]Department of Neurosurgery, Kitano Hospital, Osaka and [8]Department of Neurosurgery, Hiroshima University School of Medicine, Hiroshima, Japan

Received June 24, 2008; accepted August 14, 2008

A multicenter phase I clinical trial, namely, Integrated Japanese Multicenter Clinical Trial: A Phase I Study of Interferon-β and Temozolomide for Glioma in Combination with Radiotherapy (INTEGRA Study), is being conducted for patients with high-grade glioma in order to evaluate the safety, feasibility and preliminary clinical effectiveness of the combination of interferon-β and temozolomide. The primary endpoint is incidence of adverse events. The secondary endpoints are progression-free survival time and overall survival time. In addition, objective tumor response will be evaluated in a subpopulation of patients with the measurable disease. The reduction rate of tumor will be calculated according to Response Evaluation Criteria In Solid Tumors for measurable tumors as determined by magnetic resonance imaging. Subsequently, the overall response will be evaluated based on the results of measurable and non-measurable tumors. Ten newly diagnosed and 10 recurrent patients will be enrolled in this study.

Key words: chemo-phase I-II-III – clinical trials – CNS

INTRODUCTION

Gliomas account for ~40% of all brain tumors and are thus the most common primary tumors of the central nervous system. Primary brain tumors are classified according to their cell type and histological grade into categories defined by the World Health Organization (WHO) (1). High-grade (WHO grades III and IV) gliomas, which include anaplastic astrocytoma (AA), anaplastic oligodendroglioma (AO), anaplastic oligoastrocytoma (AOA) and glioblastoma multiforme (GBM), are often resistant to treatment; GBM, the most common glioma in adults, kills patients within a median time span of a year after diagnosis despite treatment with aggressive surgical resection, nitrosourea-based chemotherapy and radiotherapy (2–4). A number of studies by large cooperative groups have shown the benefits of radiation therapy in doses up to 60 Gy after surgery for improving overall survival and time to progression (5). In Japan, nitrosourea agents such as 1-(4-amino-2-methyl-5-pyridiminyl)methyl-3-(2-chloroethyl)-3-nitrosourea and methyl-6-[3-(2-chloroethyl)-3-nitrosoureido]-6-deoxy-alpha-D-glucopyranoside have been used to treat malignant gliomas for a long time; however, this treatment offered few clinical benefits. Temozolomide (TMZ), an oral alkylating agent, has been demonstrated to possess antitumor activity against malignant gliomas, with minimal additional toxicity; furthermore, in a previous study of concomitant radiation therapy and chemotherapy with TMZ followed by adjuvant TMZ, survival duration substantially improved (6). In 2006, TMZ

For reprints and all correspondence: Toshihiko Wakabayashi, Department of Neurosurgery, Nagoya University School of Medicine, Nagoya, Japan.
E-mail: wakabat@med.nagoya-u.ac.jp

was certified as the treatment agent for malignant gliomas by the National Ministry of Health and Welfare of Japan, and a combination of radiotherapy and chemotherapy with TMZ is now used as the first-line therapy. However, its clinical outcomes depend on the *O*-(6)-methylguanine-DNA methyltransferase (MGMT) status, and MGMT modification is one of the key factors to obtain greater clinical benefits in the future.

Interferon-β (IFN-β) exhibits pleiotropic biological effects and has been widely used either alone or in combination with other antitumor agents in the treatment of malignant gliomas and melanomas (7). In the treatment of malignant gliomas, IFN-β can act as a drug sensitizer, enhancing toxicity against various neoplasms when administered in combination with nitrosourea. IFN-β and nitrosourea combination therapy has been particularly used for the treatment of gliomas in Japan (8). Previously, we demonstrated that IFN-β markedly enhanced chemosensitivity to TMZ in an *in vitro* study of human glioma cells (9); this finding suggested that one of the major mechanisms by which IFN-β enhances chemosensitivity is the downregulation of MGMT transcription via *p53* induction. This effect was also observed in an experimental animal model (10). These two studies suggested that chemotherapy with IFN-β and TMZ plus radiation might further improve the clinical outcome in malignant gliomas when compared with TMZ plus radiation therapy. Here, in order to evaluate the safety, feasibility and preliminary clinical effectiveness of the combination of IFN-β and TMZ, we are conducting a clinical study, namely, Integrated Japanese Multicenter Clinical Trial: A Phase I Study of Interferon-β and Temozolomide for Glioma in Combination with Radiotherapy (INTEGRA study). This study involves eight medical institutions, covering the entire regional population of Japan.

PROTOCOL DIGEST OF THE STUDY

Purpose

The main aim of this study is to evaluate the safety, feasibility and preliminary clinical effectiveness of IFN-β and TMZ for the treatment of malignant gliomas.

Study Setting and Protocol Review

This is a multicenter clinical trial involving eight neurosurgical institutions: Yamagata, Saitama Medical, Nippon Medical, Nagoya, Osaka, Kyoto, and Hiroshima Universities and Kitano Hospital. The protocol has been reviewed and approved by institutional review boards of each of these institutions.

Registration and Monitoring

Participating investigators are instructed to send an eligibility criteria report to the Data Center at Nagoya University, which is a third party different from the study director. Ten newly diagnosed and 10 recurrent patients are registered for a period of 6 months from December 2007. Data, including those of magnetic resonance imaging (MRI), blood tests, and pathology, will be collected at the data center. The quality of data will be checked and verified at the data center. If required, the data center would provide feedback to the institutions. The data center will send high-quality data to the study director. Committees of safety and efficacy (Dr Kazuo Tabuchi, Koyanagi Memorial Hospital, Saga), radiotherapy (Dr Shinji Naganawa, Department of Radiology, Nagoya University School of Medicine), pathological review (Dr Youichi Nagasato, Department of Pathology, Gunma University School of Medicine) and statistics (Dr Kunihiko Hayashi, Gunma University School of Health Science) will send their reports to the head office.

Endpoints

The primary endpoint is incidence of adverse events. The secondary endpoints are progression-free survival time and overall survival time. In addition, objective tumor response will be evaluated in a subpopulation of patients with measurable disease. The reduction rate of tumor will be calculated according to Response Evaluation Criteria In Solid Tumors for measurable tumors as determined by MRI. Non-measurable tumors are classified into four grades: complete remission, partial response, progression and not evaluable. Subsequently, the overall response will be evaluated based on the results of measurable and non-measurable tumors.

Eligibility Criteria

The eligibility criteria are as follows:

(i) Histologically confirmed diagnosis of newly diagnosed or recurrent high-grade glioma (AA, AO, AOA or GBM). More than 50% volume of tumor is located in the supratentorial region.
(ii) No tumor recognized in the optic nerve, olfactory nerve and pituitary gland on pretreatment MRI.
(iii) No dissemination detected by MRI. Age between 18 and 75 years at the time of registration.
(iv) Performance status is 0–2, 3 only due to neurological deficits.
(v) Sufficient organ function before chemotherapy according to the following laboratory data: WBC $\geq 3000/mm^3$ or neutrophils $\geq 1500/mm^3$, platelets $\geq 100\,000/mm^3$, hemoglobin ≥ 8.0 g/dl, bilirubin ≤ 1.5 mg/dl, serum glutamic oxaloacetic transaminase ≤ 100 IU, serum glutamic pyruvic transaminase ≤ 100 IU, creatinine ≤ 1.5 mg/dl, creatinine clearance ≥ 50 ml/min and electrocardiogram showing no serious arrhythmia and no serious ischemic heart disease.
(vi) No prior chemoradiotherapy for newly diagnosed patients.

(vii) The interval from the end of prior anti-tumor therapy (e.g. chemotherapy, radiotherapy, immunotherapy) must be at least 4 weeks for recurrent patients, regardless of the regimen.
(viii) Written informed consent.

Exclusion Criteria

The exclusion criteria are as follows:

(i) synchronous double cancer or metachronous double cancer in last 5 years; carcinoma *in situ* accepted;
(ii) meningitis or pneumonia;
(iii) pregnant, possibly pregnant, or nursing women;
(iv) mental disorder;
(v) uncontrolled diabetes mellitus (DM) or under treatment with insulin for DM;
(vi) myocardial infarction in last 3 months;
(vii) history of pulmonary fibrosis or interstitial pneumonia.

Treatment Methods

For newly diagnosed patients:

Radiotherapy	60 Gy/30 fr, 2 Gy ×5 days/week;
IFN-β	3 MIU/body, administered intravenously on alternate days during radiotherapy;
TMZ	75 mg/(m^2 day), daily from the first day to the last day of radiotherapy.

After completing this induction period, all patients will have 4 weeks of washout period, and they will be then shifted to adjuvant period.

IFN-β	3 MIU/body, administered on the first day morning every 4 weeks;
TMZ	150 mg/(m^2 day) (days 1–5: first cycle); 200 mg/(m^2 day) (days 1–5: second to sixth cycle).

In the absence of hematologic toxicity, the dose is increased to 200 mg/(m^2 day), beginning with the second cycle to the sixth cycle.

This cycle is repeated six times every 28 days in the absence of tumor progression, serious adverse events such as grade 4 hematological toxicity, refusal of therapy and deviation from the protocol.

For recurrent patients:

IFN-β	3 MIU/body, administered the first day morning every 4 weeks (day 1);
TMZ	150 mg/(m^2 day) (days 1–5: first cycle); 200 mg/(m^2 day) (days 1–5: second to sixth cycle).

In the absence of hematologic toxicity, the dose is increased to 200 mg/(m^2 day), beginning with the second cycle to the sixth cycle.

This cycle is repeated six times every 28 days.

This regimen has been considered to be the most promising based on previous clinical studies (8,11–14). Thus, dose-limiting toxicity was not evaluated in this study.

Follow-up and Statistical Methods

Disease progression and occurrence of new disease will be examined by MRI performed at baseline and at least after every 4–5 weeks during treatment. Blood tests and symptom checks will be carried out before treatment and at least after every 2 weeks during treatment. Follow-up will continue for 3 months from the end of treatment. In cases wherein therapy is discontinued due to toxicity, clinicians would follow-up patients until they recover from toxicity. In addition, overall survival, progression-free survival and treatment success curves are constructed as time-to-event plots by the Kaplan–Meier method.

Acknowledgement

We would like to thank Dr Junichi Sakamoto for his helpful comments and suggestions.

Funding

This work was supported in part by Japan Brain Foundation.

Conflict of interest statement

None declared.

References

1. Louis DN, Ohgaki H, Wiestler OD, Cavenee WK, Burger PC, Jouvet A, et al. The 2007 WHO classification of tumours of the central nervous system. *Acta Neuropathol* 2007;114:97–109.
2. Nagane M, Levitzki A, Gazit A, Cavenee WK, Huang HJ. Drug resistance of human glioblastoma cells conferred by a tumor-specific mutant epidermal growth factor receptor through modulation of Bcl-XL and caspase-3-like proteases. *Proc Nat Acad Sci USA* 1998;95:5724–9.
3. Ohgaki H, Dessen P, Jourde B, Horstmann S, Nishikawa T, Di Patre PL, et al. Genetic pathways to glioblastoma: a population-based study. *Cancer Res* 2004;64:6892–9.
4. Ohgaki H, Kleihues P. Population-based studies on incidence, survival rates, and genetic alterations in astrocytic and oligodendroglial gliomas. *J Neuropathol Exp Neurol* 2005;64:479–89.
5. Walker MD, Green SB, Byar DP, Alexander E Jr, Batzdorf U, Brooks WH, et al. Randomized comparisons of radiotherapy and nitrosoureas for the treatment of malignant glioma after surgery. *N Engl J Med* 1980;303:1323–9.
6. Stupp R, Mason WP, van den Bent MJ, Weller M, Fisher B, Taphoorn MJ, et al. Radiotherapy plus concomitant and adjuvant temozolomide for glioblastoma. *N Engl J Med* 2005;352:987–96.
7. Chawla-Sarkar M, Lindner DJ, Liu YF, Williams BR, Sen GC, Silverman RH, et al. Apoptosis and interferons: role of interferon-stimulated genes as mediators of apoptosis. *Apoptosis* 2003;8:237–49.
8. Wakabayashi T, Hatano N, Kajita Y, Yoshida T, Mizuno M, Taniguchi K, et al. Initial and maintenance combination treatment with interferon-beta, MCNU (Ranimustine), and radiotherapy for patients with previously untreated malignant glioma. *J Neurooncol* 2000;49:57–62.